FREQUENCY-SELECTIVE LIMITER AND ITS APPLICATION IN A FILTER BANK RECEIVER

Rex C. S Chien

Massachusetts Institute of Technology

Prepared for:

Electronic Systems Division

13 April 1973

MASSACHUSETTS INSTITUTE OF TECHNOLOGY

LINCOLN LABORATORY

FREQUENCY-SELECTIVE LIMITER AND ITS APPLICATION IN A FILTER BANK RECEIVER

R. C. S. CHIEN

Group 91

TECHNICAL NOTE 1973-1

13 APRIL 1973

LEXINGTON MASSACHUSETTS

The work reported in this document was performed at Lincoln Laboratory, a center for research operated by Massachusetts Institute of Technology, with the support of the Department of the Air Force under Contract F19628-73-C-0002.

DOCUMENT CONTROL DATA - R&D

(Security classification of title, body of abstract and indexing annotation must be entered when the overall report is classified)

1. ORIGINATING ACTIVITY *(Corporate author)* Lincoln Laboratory, M.I.T.	2a. REPORT SECURITY CLASSIFICATION Unclassified 2b. GROUP None

3. REPORT TITLE

Frequency-Selective Limiter and Its Application in a Filter Bank Receiver

4. DESCRIPTIVE NOTES *(Type of report and inclusive dates)*

Technical Note

5. AUTHOR(S) *(Last name, first name, initial)*

Chien, Rex C. S.

6. REPORT DATE	7a. TOTAL NO. OF PAGES	7b. NO. OF REFS
13 April 1973	62	12

8a. CONTRACT OR GRANT NO. F19628-73-C-0002 b. PROJECT NO. 627A c. d.	9a. ORIGINATOR'S REPORT NUMBER(S) Technical Note 1973-1 9b. OTHER REPORT NO(S) *(Any other numbers that may be assigned this report)* ESD-TR-73-81

10. AVAILABILITY/LIMITATION NOTICES

Approved for public release; distribution unlimited.

11. SUPPLEMENTARY NOTES	12. SPONSORING MILITARY ACTIVITY
None	Air Force Systems Command, USAF

13. ABSTRACT

One important requirement in the implementation of responsive countermeasures is to be able to sense the electronic order of battle. This technique can have application to many classes of countermeasures such as jamming, masking, communications or homing. The process of sensing the electromagnetic spectrum requires the ability to select a narrow portion of the spectrum and evaluate the signals present. One method to do this is with a bank of filters. There is, however, a common difficulty encountered in building the filter bank, that is the extremely high roll-off rate required of the bandpass filters to reject the strong out-of-band signals. This stringent requirement imposes a highly complicated design on the filter bank.

One solution is to reduce the complexity of the filter bank by normalizing the signal levels by a frequency-selective limiter (FSL). By normalizing all signal levels at an equal amplitude before feeding them into the filter bank, the necessity of constructing bandpass filters with high rejection rates can be greatly reduced.

The operating theory of parametric FSL's and the measured results of a yttrium iron garnet (YIG) FSL under different signal environments are reported. Emphasis is given to application YIG FSL's as level normalizers in a filter bank receiver.

YIG FSL operation is discussed via a basic analytical model. In this study, transient response to pulsed RF signals, frequency modulated signals, small signal suppression and intermodulation product phenomena when two signals are simultaneously received, are also reported.

Experimental results obtained agree with the analytical model. Extensive data are provided to facilitate design of YIG FSL's in filter bank receivers.

Specific applications for YIG FSL's are presented: YIG FSL as a level normalizer, cascading YIG FSL's to obtain large limiting range, threshold level detection influenced by small signal suppression, and use of a YIG FSL to offset amplitude reduction of bandpass filters caused by a sweep signal.

A filter bank receiver comprising YIG FSL's is presently under construction.

14. KEY WORDS

frequency-selective limiter
filter bank receiver
satellite communications
re-entry systems
YIG

Specific applications for YIG FSL's are presented: YIG FSL as a level normalizer, cascading YIG FSL's to obtain large limiting range, threshold level detection influenced by small signal suppression, and use of a YIG FSL to offset amplitude reduction of bandpass filters caused by a sweep signal.

A filter bank receiver comprising YIG FSL's is presently under construction.

Accepted for the Air Force
Joseph J. Whelan, USAF
Acting Chief, Lincoln Laboratory Liaison Office

CONTENTS

CONTENTS (Continued)

INTRODUCTION

Although interesting applications of yttrium iron garnet (YIG) frequency-selective limiters (FSL's) have been reported in the literature during the past decade, their value as a building block in communication systems has received only nominal attention. FSL's tend not to be "captured" by strong signals, and the intermodulation products are generally negligible in the presence of more than one signal. Such characteristics could be used advantageously in an ECM receiver system (Fig. 1) that uses a large number of contiguous bandpass filters to detect and identify the frequencies of received signals. (Generally, the absolute strengths at the outputs are of no interest.) Once the level of a signal reaches a preset threshold, the trigger circuit is initiated to record incoming signals and their frequencies corresponding to positions of the filters.

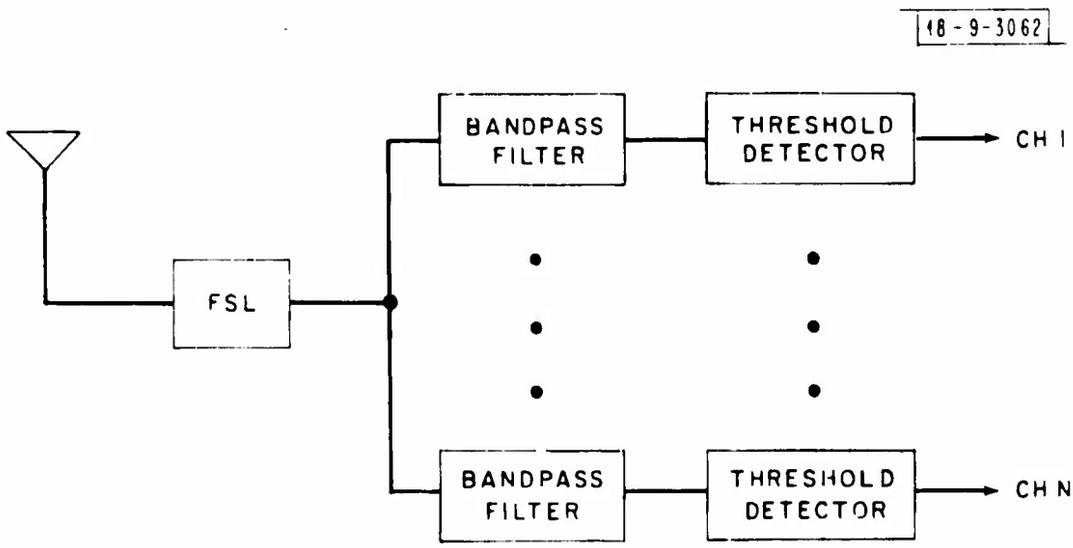

Fig. 1. Filter bank receiver.

One difficulty encountered in building the filter bank is the extremely high roll-off rate required of the bandpass filters. Consider a wide range of signal levels

applied to a bandpass filter with finite roll-off rate; if the threshold is set to detect the smallest in-band signal desired, then a large signal whose signal frequency falls outside the passband could also reach the threshold and trigger the output circuits. An extremely strong signal could trigger many channels and disable the system.

A straightforward solution is to build bandpass filters that contain many stages. The more poles there are in the bandpass filters, the higher the roll-off rate that can be obtained. However, the total number of stages of the filter bank will be equal to the number of stages times the number of channels of the filter bank. Complexity, size and weight are therefore multiplied.

A solution to the problem is to normalize the signal levels by FSL's before they are fed into the filter bank. If signals fed into the filter bank possess equal amplitude, out-of-band triggering can be prevented by setting the threshold at the intersection point of the bandpass filters. Ideally, normalized signals can be identified with the simplest one-pole filter bank. As a result, high roll-off rate is no longer necessary and the complexity of the filter bank can be greatly reduced.

The FSL can be considered as a device whose input signal levels (Fig. 2) are large

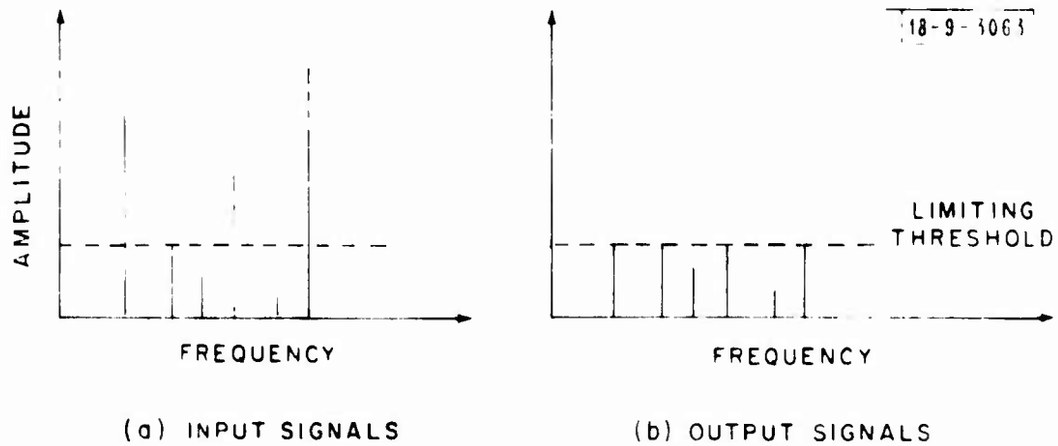

Fig. 2. I L (a) input and (b) output signal level.

and diverse, whereas the output signals are normalized with respect to the limiting threshold. Consequently, the FSL is a self-adaptive device that will normalize levels on a frequency-by-frequency basis.

FSL devices with these characteristics have been constructed in various types: magnetoelastic,[1] nuclear magnetic,[2] electron paramagnetic,[3] and spin-wave. Only the spin-wave mode of a YIG sphere is practical and most attractive in terms of simplicity of construction, size, weight and performance.

The purpose of this report is to present the operating theory and measurement results for a YIG FSL under different signal environments. Application of the YIG FSL in a filter bank receiver for signal spectrum identification is emphasized, but the measurement results are applicable to other types of systems such as multi-channel satellite communications and anti-jamming receivers.

Operation of the YIG FSL is discussed in Section I via analytical models. Measurement of 1) power distribution, 2) leakage spike, 3) small signal suppression, 4) intermodulation (IM) products, and 5) linear frequency modulation response are presented in Section II. Section III deals with applications of the YIG FSL as a level normalizer with particular attention to: 1) cascading YIG FSL to obtain large limiting range, 2) 3rd order IM products, 3) small signal suppression and threshold level detector, and 4) response of a YIG FSL filter bank receiver to a linear FM signal.

I. Operation of a Parametric FSL

A. Basic Models

The basic analytical model of a parametric limiter was developed and analyzed by Ho and Siegman.[4] Their primary interest was to use the limiter's phase distortionless characteristics. This model permits qualitative explanation of basic YIG FSL operation, and in a restricted manner, (because of the lack of basic YIG FSL parameters) its numerical analysis.[5, 6]

Two resonant tanks of frequency ω and $\omega/2$ are coupled by a nonlinear element in what is basically a parametric oscillator (Fig. 3). Input power is coupled to the ω tank as is the output power.

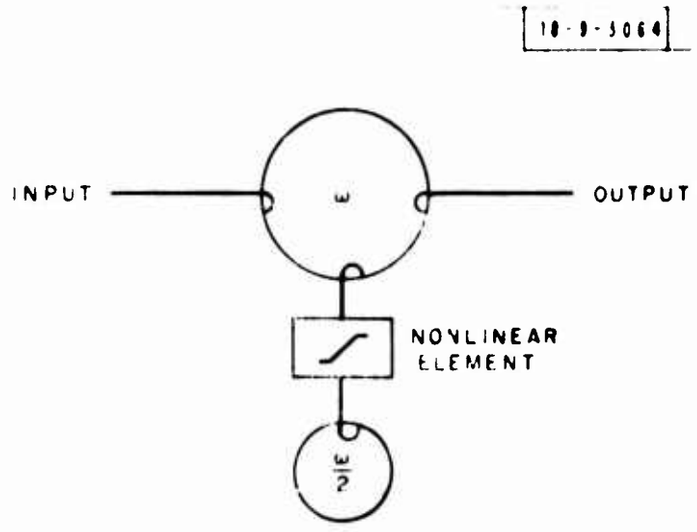

Fig. 3. Subharmonic oscillation limiter.

When an input signal at frequency ω is below a certain threshold, it will pass through the ω tank as if subharmonic tank $\omega/2$ did not exist, and therefore, no subharmonic oscillation existed in the $\omega/2$ tank. However, when the input power is above threshold power P_{th}, oscillation will be excited at a frequency exactly half the input frequency. The result is that part of the input power is transferred to maintain the subharmonic oscillation, and part is reflected to the input source because of the impedance mismatch caused by the added equivalent conductance to ω tank caused by oscillation in the $\omega/2$ tank. These combined effects result in a sharp limiting characteristic (Fig. 4). As input power increases, subharmonic oscillation continues to increase, but output power remains constant.

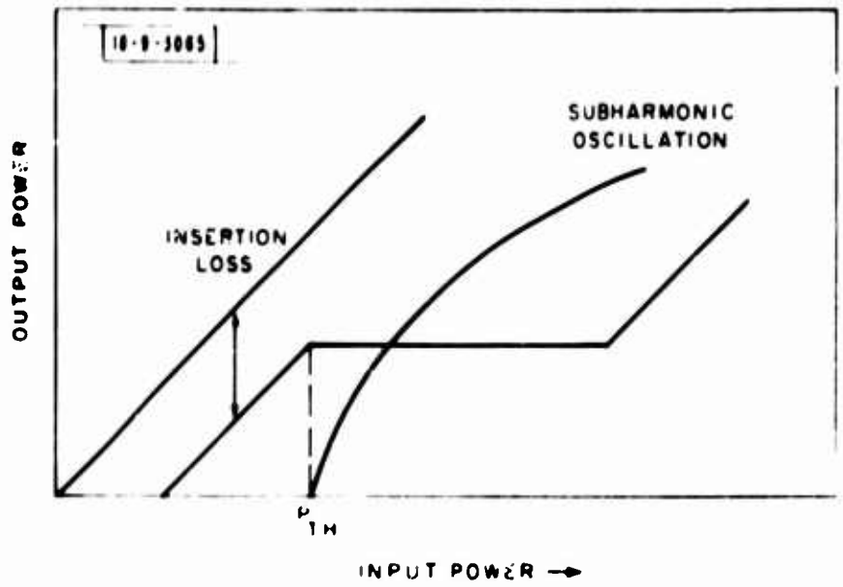

Fig. 4. Subharmonic oscillation and limiting characteristics.

This concept permits development of an FSL model (Fig. 5) that has an ω tank with large bandwidth, B, with a bank of subharmonic tanks coupled to the ω tank. If the

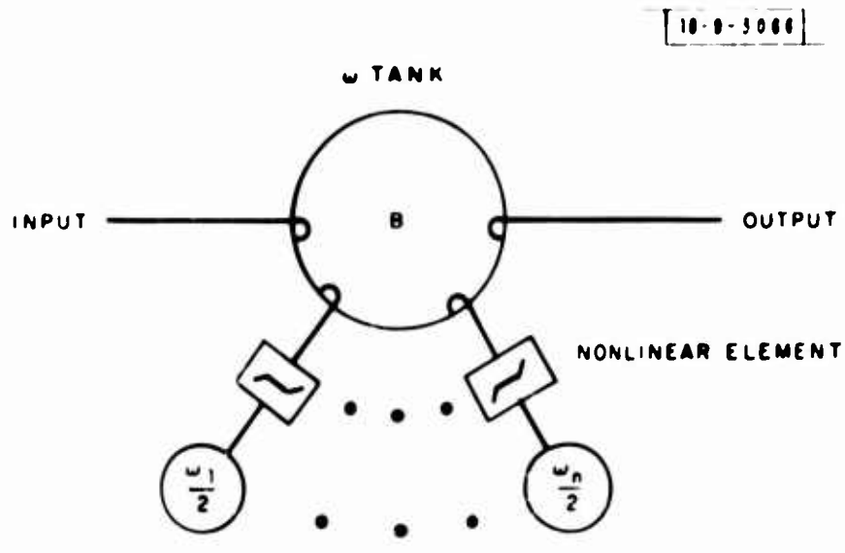

Fig. 5. Frequency-selective limiter model.

subharmonic tanks are tuned contiguously in frequency across the bandwidth, B/2, an FSL is formed. Thus, when the input signal in bandwidth B is smaller than threshold P_{th}, the ω tank can be considered as an ordinary resonant tank inserted between the input and output. However, when the signal at ω_1 is above P_{th}, the corresponding subharmonic tanks, $\omega_1/2$, will be excited into oscillation. Hence, one finds that each subharmonic tank reacts at only twice its resonant frequency (or at a small bandwidth centered at ω_1). Frequencies separated by bandwidth ω_1 will be mutually independent because their half frequencies do not fall in the same subharmonic tank. Consequently, limiting is done on a frequency-by-frequency basis.

B. Circuit Model

The parametric limiter can be demonstrated successfully by a circuit model (Fig. 6) in the VHF band. The circuit uses a varactor as the nonlinear

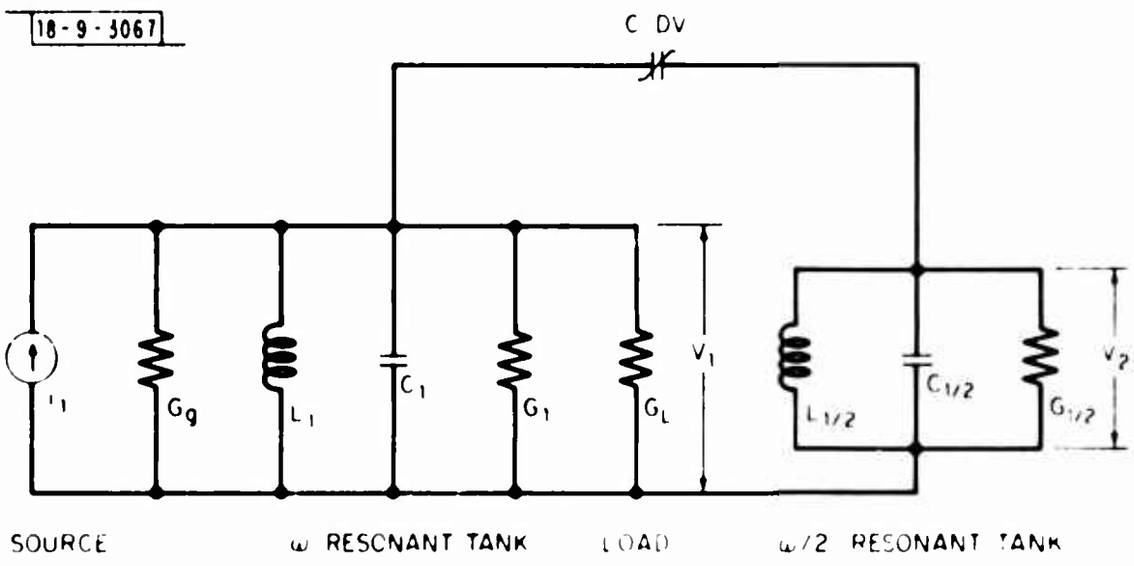

Fig. 6. Circuit model for varactor diode parametric limiter.

coupling element between the ω and $\omega/2$ resonant tanks. When the $\omega/2$ tank is tuned to exactly half the resonant frequency of the ω tank, and the input signal is at the

center frequency of the ω resonant circuit, the circuit can be analyzed by solving differential equations describing the model:

$$\frac{dV_1}{dt} + \frac{\omega}{2Q_T} V_1 + j \frac{\omega D}{2C_1} V_{1/2}^2 = \frac{I_1}{2C_1} + j \frac{1}{2\omega C_1} \frac{dI_1}{dt} \tag{1}$$

$$\frac{dV_{1/2}}{dt} + \frac{\omega}{4Q_{1/2}} V_{1/2} + j \frac{\omega D}{2C_{1/2}} V_{1/2}^* V_1 = 0, \tag{2}$$

where

$V_1 = V_1(t) \exp[j\omega t] + V_1^*(t) \exp[-j\omega t]$

$V_{1/2} = V_{1/2}(t) \exp\left[\frac{j\omega t}{2}\right] + V_{1/2}^*(t) \exp\left[-\frac{j\omega t}{2}\right]$

$V = V_1 + V_{1/2}$

$G_T = G_g + G_1 + G_L$

$Q_T = \frac{\omega C_1}{G_T}$

$Q_{1/2} = \frac{\omega C_{1/2}}{2G_{1/2}}$

D = First order nonlinear coefficient of varactor.

The steady state solution may be obtained by allowing the time derivative terms to be zero:

$$I_{th} = -\frac{G_T G_{1/2}}{\omega D} \tag{3}$$

$$V_1 = j \frac{G_{1/2}}{\omega D} \frac{V_{1/2}}{V_{1/2}^*}. \tag{4}$$

Equation (3) defines the threshold magnitude, I_{th}, of input current, I_1, which will cause subharmonic oscillation. When the input current is larger than I_{th}, the output will be limited. Equation (4) shows that the magnitude of output voltage V_1 is independent of the input current I_1 as well as $V_{1/2}$ when V_1 is limited.

Equations (1) and (2) are also useful in analyzing the transient responses. The YIG limiter exhibits a large leakage spike when a pulsed RF signal above the limiting level is applied. The leakage is usually not desired and causes troublesome effects in most applications. The mechanism forming the leakage spike can be explained.

When an input pulse with steep leading edge is applied to the limiter (Fig. 7) the subharmonic oscillation starts immediately to build up from the noise level toward its

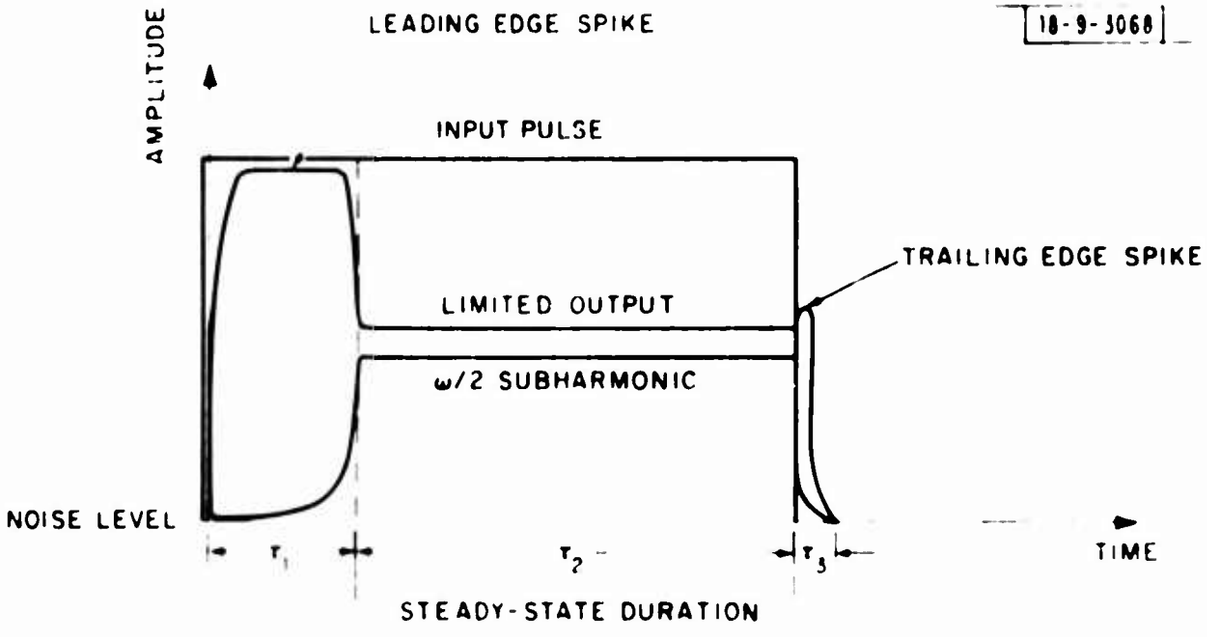

Fig. 7. Leading edge spike, trailing edge spike and subharmonic build up when input is a pulse function.

steady state level. The subharmonic buildup is an exponential function of time. The rate of rise of the $\omega/2$ oscillation depends on, among other factors, the input level relative to the threshold power of the limiter. Before the $\omega/2$ oscillation reaches the steady state level, limiting does not occur. The input signal will pass through the limiter and appear at the output with full amplitude. When the subharmonic oscillation has built up to the steady state, the output drops instantaneously to the limited level. Hence a leading edge spike is formed. The duration of the spike can also be obtained from Eqs. (1) and (2) and is given as

$$\tau_1 = \frac{2Q_{1/2}}{(n-1)\omega} \ln\left(\frac{P_{ss}}{P_n}\right) \tag{5}$$

where

P_{ss} = steady state subharmonic power level

P_n = noise power level of subharmonic tank

$n = \sqrt{P/P_{th}}$

P = input power

P_{th} = threshold power.

The value of $\ln (P_{ss}/P_n)$ is a relatively large number since P_n is at the noise power level. Variation of P_{ss} contributes less to τ_1 than n; therefore, the spike duration, τ_1, is strongly dependent on n when $Q_{1/2}$ and ω are usually determined by the spin-wave line width of the YIG material and the operating frequency.

The trailing spike, with no amplitude significance is generated by turning off the input signal when the subharmonic oscillation reaches steady state. Some of the stored energy in the $\omega/2$ tank reconverts to the ω frequency and appears at the output when the signal, ω, is turned off. Trailing edge spikes are not observed in YIG

FSL measurements.

As the input pulse becomes narrower, the steady state duration τ_2 approaches zero. Output power is then not limited at all. The time $\tau_1 + \tau_3$ is a good approximation of the response time to an impulse function at input. In fact, due to the negligible effect of the trailing edge spike, the impulse response can be given by τ_1.

For an input pulse with duration σ shorter than the spike duration τ_1, higher power than P_{th} is needed to see the limiting affect. Equation (5) can be solved for the input power needed to reach the limiting threshold:

$$P = P_{th} \left[\frac{2Q}{\omega \sigma} \right]^{1/2} \ln \left(\frac{P_{ss}}{P_n} \right) - 1 \Bigg]^{1/2} . \qquad (6)$$

Where σ has been substituted for τ_1; the smaller the value for σ, the more input power is needed. The excess power is used to speed up the subharmonic oscillation to the steady state value, hence limiting can result.

C. YIG FSL

A large number of subharmonic tanks are needed to implement an FSL as shown in Fig. 5, since selectivity is dependent on the number of $\lambda/2$ tanks across a certain bandwidth. The same difficulties as building the filter bank would be encountered if one had to construct a large number of contiguously tuned, high-Q, resonant circuits. However, the YIG limiter is seen to closely approximate the FSL model as it possesses a large number of closely spaced high-Q, spin-wave modes wher the limiter is operated in the coincidence-limiting mode. Kotzebue[7] demonstrates the independent limiting characteristic of a YIG FSL and describes its operation via an FSL model.

Although the spin-waves are the substitution of the $\lambda/2$ resonant tanks in the YIG FSL, the behavior of the YIG FSL can be predicted by the circuit model and fundamental

theory just derived. In practice, because of finite selectivity, $Q_{1/2}$, of the sub-harmonic tanks (spin-wave line width), independent limiting of signals can be observed only when signals are separated in frequencies larger than the spin-wave line width. When the separation between signals is small, some undesired nonlinear effects are generated at the output; namely, intermodulation products and small signal suppression. These nonlinear effects are strongly dependent on frequency separation as well as the input power level.

Intermodulation products represent a false signal at the output of the filter bank -- an entirely new signal that is not really received by the antenna -- and small signals can be suppressed by large limited signals. Therefore, a small signal can be suppressed below the level of the trigger circuits at the output of the filter bank.

A YIG FSL developes spike leakage as discussed when an RF signal is pulse modulated. However, it would also develope spike leakage if a CW signal is time-frequency coded so that the frequency shift is larger than the spin-wave line width. A different case from the transient spike leakage is that when a linear frequency-modulated signal is applied to a YIG FSL. The response of the YIG FSL depends on the signal sweep rate.

The aforementioned phenomena are part of the characteristics of the YIG FSL whose mechanisms are discussed next.

1. Intermodulation Products

When two signals at ω_1 and ω_2 are applied to an FSL, many intermodulation products are generated.

$$\omega_{IM} = m\omega_1 + n\omega_2 \tag{7}$$

where m and n are integers. For a particular value of m and n, the K^{th} order IM product is defined by

$$K = |m| + |n|. \tag{8}$$

Among various orders of IM products, only the ones that fall within passband, B, of the FSL have to be considered. The worst kind is found to be the 3rd order IM products.

$$\omega_{IM} = 2\omega_1 - \omega_2 \tag{9}$$

and

$$\omega_{IM} = 2\omega_2 - \omega_1 ,$$

which have the largest significant amplitude. The output spectrum (Fig. 8) shows two fundamental signals and their 3rd order IM products when ω_1 and ω_2 are 10 dB above the threshold power, P_{th}, and have 3-MHz spacing.

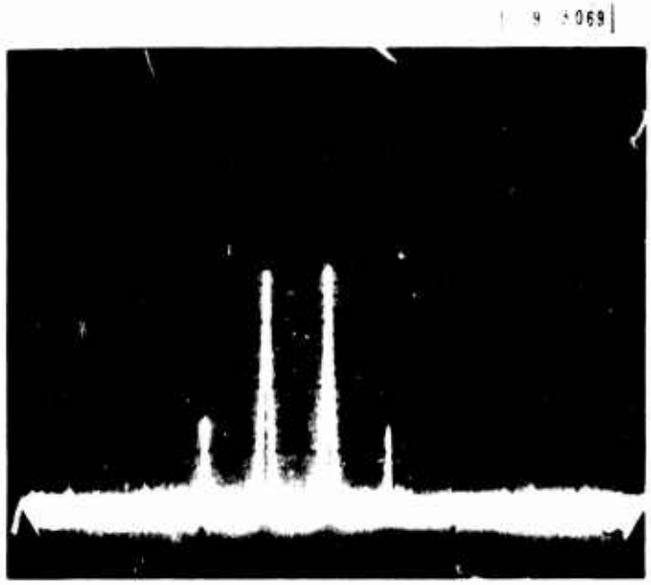

Horizontal: 3 MHz/cm
Vertical: 10 dB/cm

Fig. 8. 3rd order IM products for two equally powered signals.

The magnitude of the 3rd order products is a function of the frequency separation. For the same input power level, the amplitude of the 3rd order IM product will be

reduced rapidly as frequency separation is increased.

Exact prediction of 3rd order IM products is complicated because it is also dependent on the input power. Ciarola[6] has derived a two-signal theory (Fig. 9) 3rd order IM

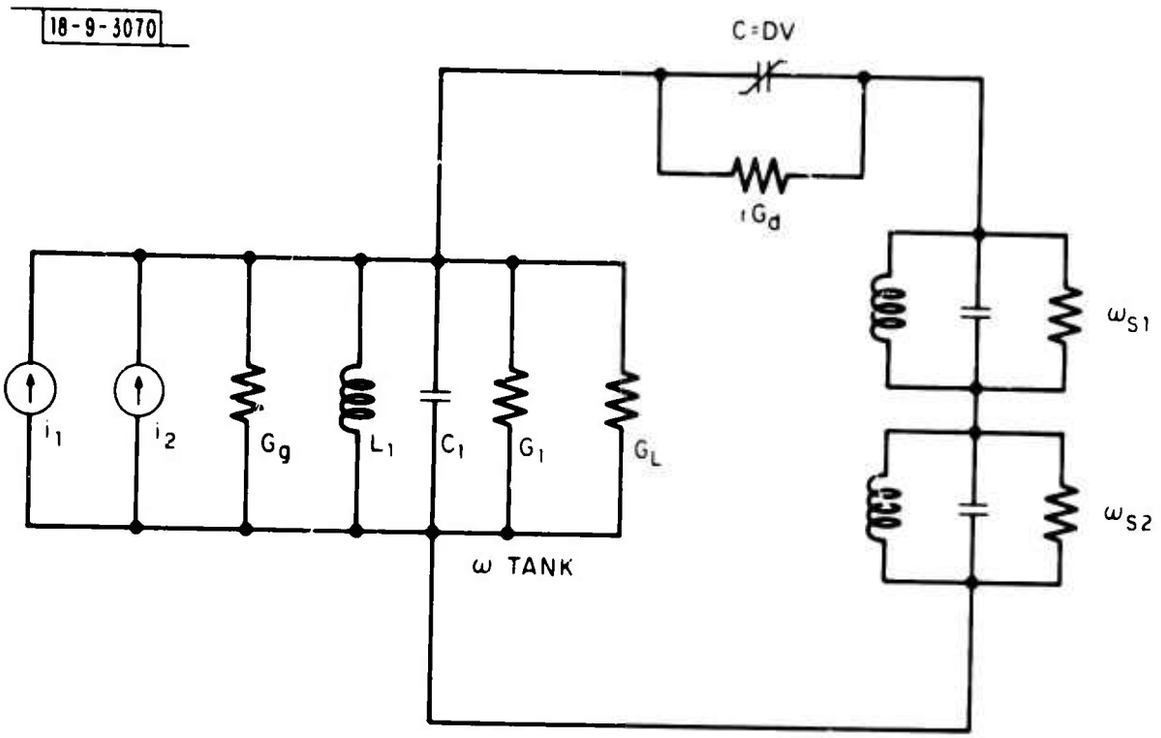

Fig. 9. Circuit model for 3rd order IM products.

product. The results are given by

$$\frac{V_{2\omega_1 - \omega_2}}{V_{\omega_1}} = \frac{2\left(\frac{|I_1|}{I_{th}} - 1\right)}{\left[2\left(\frac{|I_1|}{I_{th}}\right) - 1 - \Delta^2\right] - 2j\left(\frac{|I_1|}{I_{th}}\right)\Delta} \qquad (10)$$

where $\Delta = 2Q_{S1}\frac{\delta}{\omega_{S1}}$

$$\delta = 1/2\,(\omega_2 - \omega_1)$$

$$G_t = G_1 + G_g + G_L + rG$$

$$I_{th} = \frac{G_S G_t}{\omega_1 D}\,.$$

A plot of the magnitude of Eq. (1) as a function of the normalized frequency spacing with respect to Δ is shown in Fig. 10. The curve shows the general characteristic that the 3rd order IM magnitude is strongly dependent on frequency separation and agrees with the experimental results.

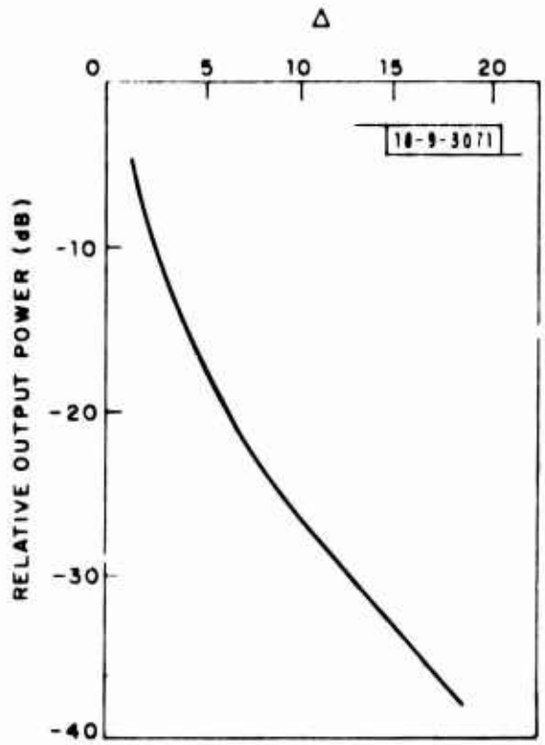

Fig. 10. 3rd order IM product for two equally powered signals each 12 dB above the limiting knee (after A. J. Giarola).

2. Small Signal Suppression

When two signals, ω_1 and ω_2, are applied to an FSL so that one signal is large enough to be limited and the other is below the threshold, P_{th}, the small signal at the output is a function of the frequency separation and the amplitude of the large signal. The result is that the small signal is suppressed in amplitude by the presence of the large signal. This effect is also generated by nonlinear behavior and is described as small signal suppression.

The amount of suppression versus frequency spacing and input power can be derived via the circuit model in Fig. 11. The model has two current sources, I_1 and I_2, fed into the ω tank. I_1 and I_2 represent the large and small signals, respectively.

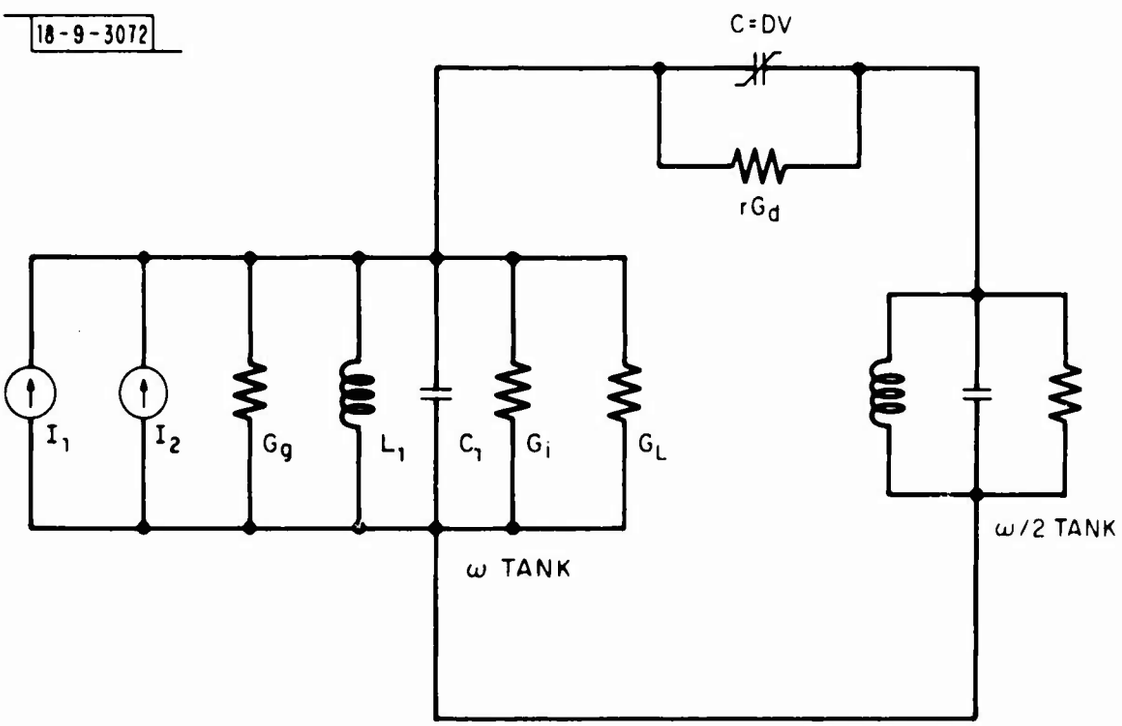

Fig. 11. Circuit model for small signal suppression.

The normalized small signal amplitude has been given by Giarola and reproduced as

$$\frac{G_t V_2}{I_2} = \frac{\left[\Delta^2 + 2\left(\frac{|I_1|}{I_{th}} - 1\right)\right] + 2j\Delta\left(\frac{|I_1|}{I_{th}}\right)}{\left[4\left(\frac{|I_1|}{I_{th}} - 1\right)\frac{|I_1|}{I_{th}} - \Delta^2\right] + 2j\Delta\left(2\frac{|I_1|}{I_{th}} - 1\right)} \quad . \tag{11}$$

The normalized 3rd order IM products in this case are given by

$$\frac{G_t V_3}{I_2} = \frac{2\left(\frac{|I_1|}{I_{th}} - 1\right)}{\left[4\left(\frac{|I_1|}{I_{th}} - 1\right)\frac{|I_1|}{I_{th}} - \Delta^2\right] - 2j\Delta\left(2\frac{|I_1|}{I_{th}} - 1\right)} \quad . \tag{12}$$

Figure 12 was obtained by using a spectrum analyzer, monitoring at the output when two signals were fed into the YIG FSL. The level of the fixed frequency at the center was 10 dB above the limiting knee, P_{th}. The variable frequency level was just below the knee. As the variable frequency was swept from left to right, the 3rd order product, $2f_2 - f_1$, swept in the opposite direction. The envelope of the small signal tracked a V-shaped curve, the valley of which coincided with the fixed large frequency to signify the small signal suppression is a function of frequency separation. The 3rd order IM product traced an inverted V curve, the peak of which coincided with the fixed frequency separation. These curves are a general description of Eqs. (11) and (12).

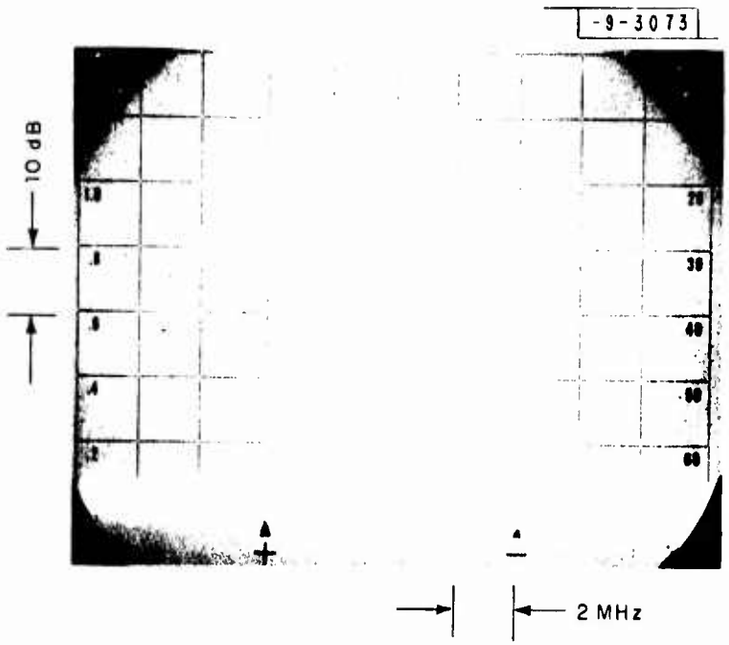

Fig. 12. 3rd order IM product and small signal suppression behavior of YIG FSL, when two signals, one on the limiting knee and one 10 dB above the limiting knee are fed into the input.

A family of V and inverted V curves can be plotted by substituting different values of large amplitude signal, I_1, into Eqs. (11) and (12). The results are plotted in Fig. 13. It is worth noting that curves derived from these equations showed two distinct points:

a. The amount of small signal suppression when the two signals approach coincidence is equal to what it would be when a conventional type limiter is used. Small signal suppression in dB = x + 6 where x is the large signal input power in dB above the limiting knee.

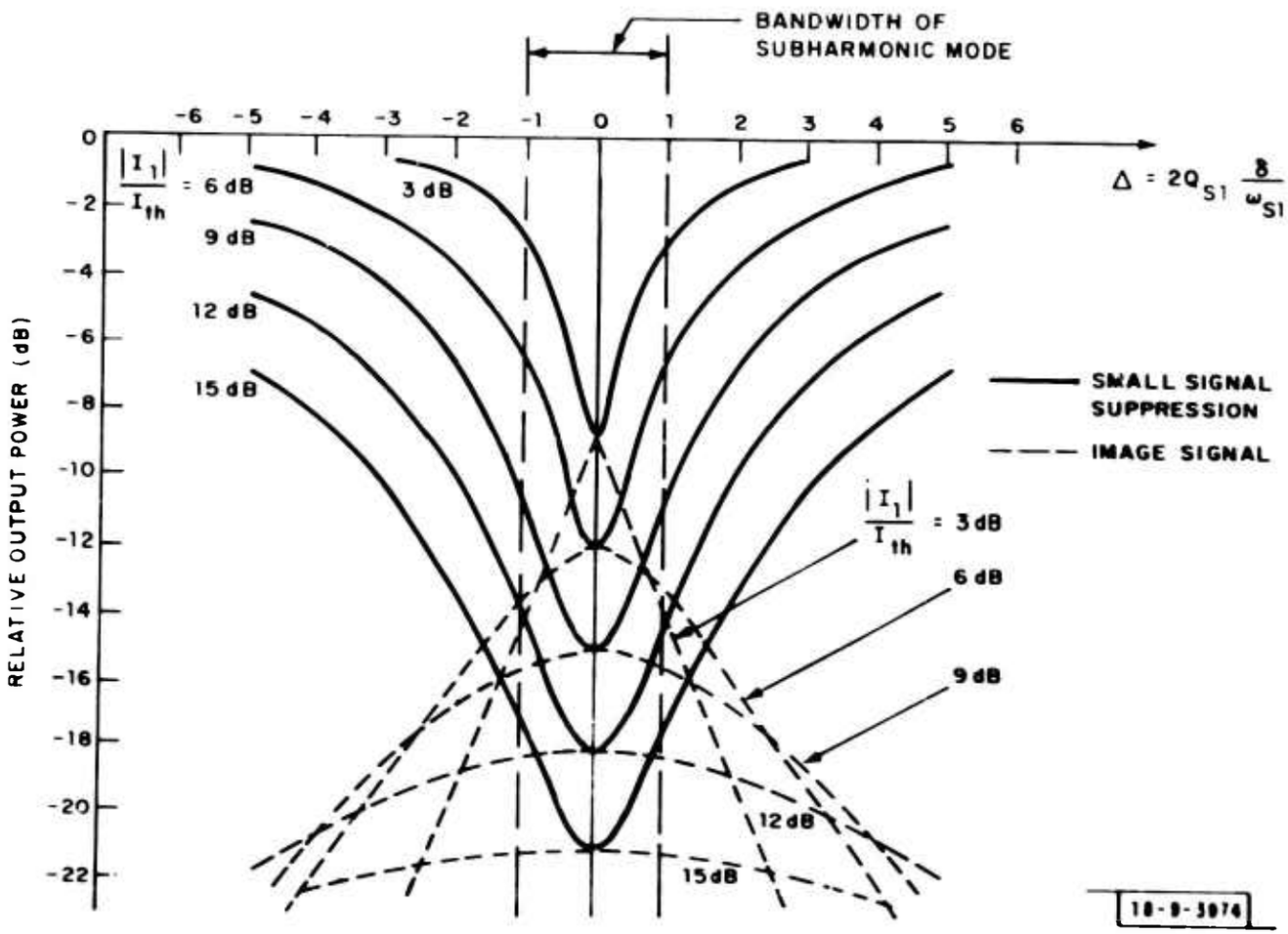

Fig. 13. Power levels of the small signal and its image as functions of the frequency separation between large and small signal. (after A. J. Giarola)

b. The amplitude of the suppressed small signal is equal to the amplitude of the 3rd order IM product when the two signals coincide. The peak of the inverted V and the valley of V curves not only coincide, but also intersect at their vertices.

3. Response to a Time-Frequency Coded CW Signal

A time-frequency coded waveform is a signal whose frequency is shifted on an interval-to-interval basis while the amplitude is a constant (Fig. 14a). When such a signal is applied to an FSL, the analysis is analogous to the transient responses described in the previous section.

Though the signal is CW, to the subharmonic tanks the time-frequency coded signal is hopping. Recall that in the FSL model the subharmonic tanks are successively tuned in frequency. Each subharmonic tank is pumped into oscillation by twice its resonant frequency. Therefore, every time the pumping frequency is shifted abruptly, and the amount of the shift is larger than the bandwidth of the subharmonic tank, the oscillation in the subharmonic tank has to start to build up from noise; this results in a delay in limiting action. The leakage spike will occur each time the frequency is shifted. Consequently, a series of comb-like leakage spikes will be received at the output (Fig. 14b).

As the frequency shifting pulse gets shorter, the duration of the signal to pump the corresponding tank is shortened, therefore, more input power is required to reach steady state. Limiting does not occur until the input power is higher then P_{th}.

4. Linear Frequency Modulation Response

A linear frequency modulation (LFM) signal is one where

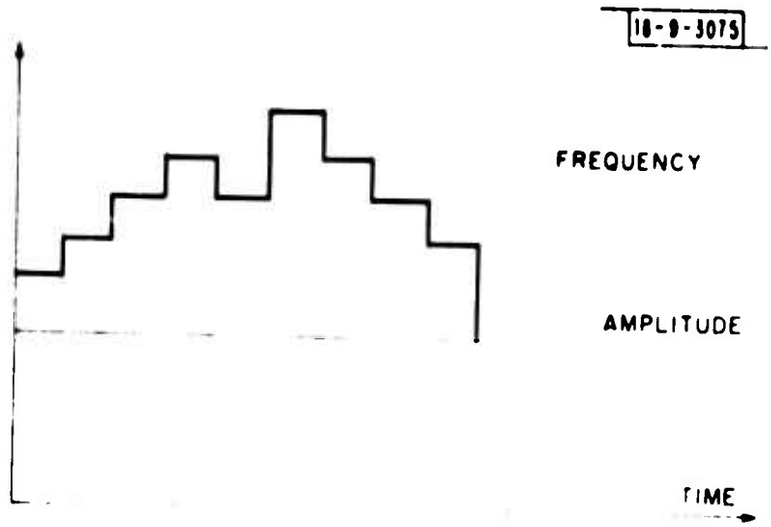

(a) TIME-FREQUENCY CODED WAVEFORM

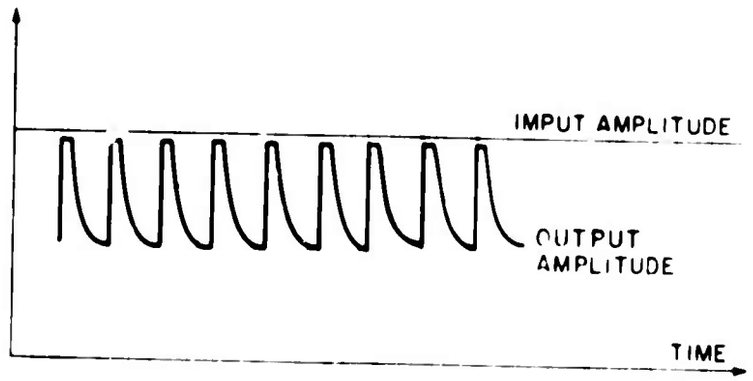

(b) INPUT AND OUTPUT RESPONSE

Fig. 14. FSL response to time-frequency coded signal.

the frequency is continuously shifting (Fig. 15). Its instantaneous frequency can be expressed as a function of time

$$\omega(t) = \omega_0 + 2\pi st \tag{13}$$

where s is the sweep rate defined as the total frequency change, F, divided by the duration, T

$$S = F/T. \tag{14}$$

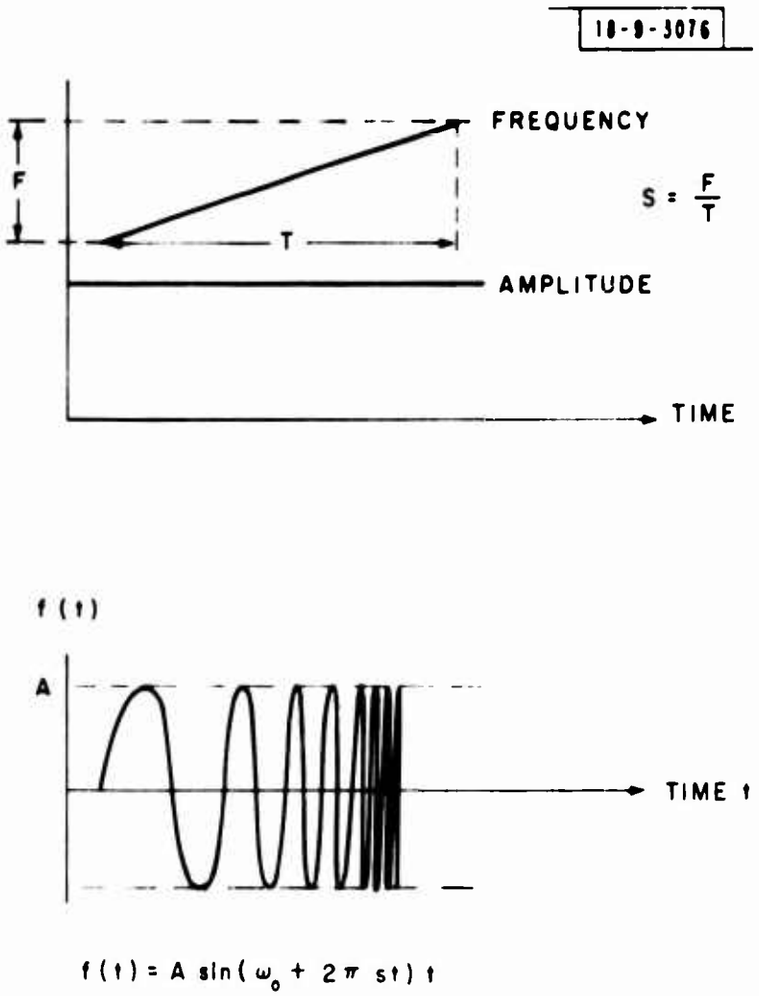

Fig. 15. Linear FM signal.

If an LFM signal is applied to the FSL, a subharmonic tank will effectively see the pumping signal sweep over the bandwidth, $\Delta f_{1/2}$, in a short time. How long the pumping signal remains in the bandwidth $\Delta f_{1/2}$ depends on the sweep rate as given by

$$d = \frac{\Delta f_{1/2}}{S/2}. \tag{15}$$

The problem here is quite similar to the well-known response of a tuned circuit to a swept frequency. Generally, the response of a bandpass filter to a swept signal depends on the sweep rate. The response is distorted by a reduction of peak amplitude when the bandpass filter is swept in time period d comparable to its rise time for the impulse response, τ. Thus, for a subharmonic tank, distortion occurs when the relation of the sweep rate, bandwidth and response time is

$$\frac{\Delta f_{1/2}}{S/2} \approx \tau. \tag{16}$$

The concept can be further simplified if the time bandwidth product, K, is introduced

$$K = \tau \cdot \Delta f_{1/2} \tag{17}$$

where K is a value usually of the order of unity, $K \sim 1$.

For a signal that is swept slowly, $S \ll 2/\tau^2$, the response of the subharmonic oscillation is essentially the response as if a CW were applied. This condition is sometimes called a quasi-state condition. The output power will be limited when the input power is larger than P_{th}, as defined by Eq. (3).

Distortion results when the swept rate is increased to $S \gg 2/\tau^2$. In this case, the pumping signal staying in the bandwidth, $\Delta f_{1/2}$, is less than the subharmonic

oscillation relaxation time τ; therefore, limiting cannot occur when input power is equal to P_{th}. Higher input power is needed to reduce the response time τ since τ is a function of input power as given by Eq. (5).

Consequently, when a sweep frequency is applied at the input, and the sweep rate is fast enough such that $S \ll 2/\tau^2$, the FSL output will not be limited to the same level as when a CW is applied. The limiter will exhibit a higher threshold power. Therefore, the threshold power level depends on the sweep rate and the selectivity, $Q_{1/2}$, of the subharmonic tanks. The higher the sweep rate and the $Q_{1/2}$, the larger the input power required to reach the threshold level -- and output power will be limited at a higher level.

II. YIG FSL Experimental Results

An experimental YIG FSL was made with four YIG spheres in series (Fig. 16),

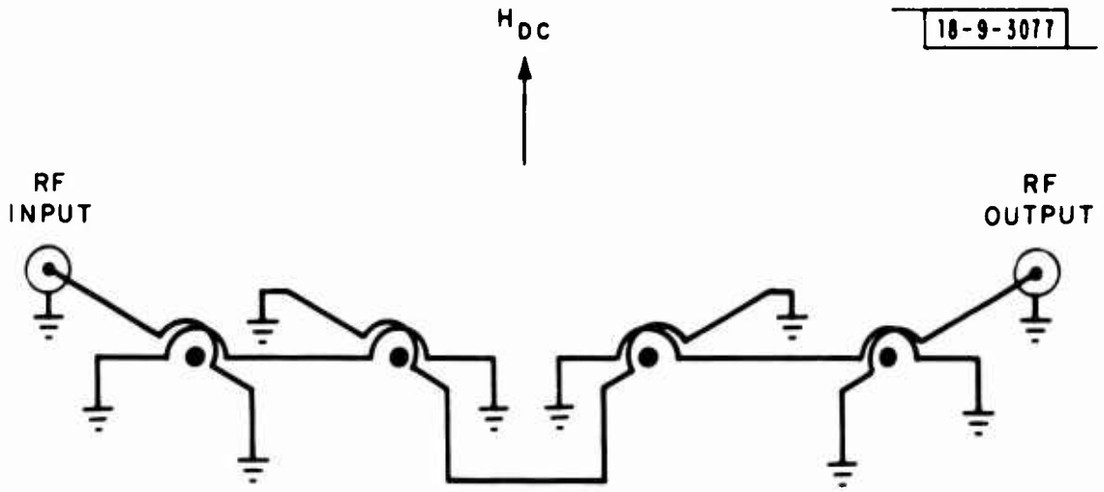

Fig. 16. Multi-stage YIG FSL.

to obtain the large limiting range required to handle large dynamic signals. The unit met the following specifications:

Frequency	S-band
Insertion loss below P_{th}	5 dB
Input limiting knee, P_{th}	-8 dBm
Limiting range	36 dB
Passband VSWR for input power = P_{th}	1.3
Volume (excluding RF connections)	0.5 in^3 (approx.)
Weight	1 oz

The unit's nominal volume (0.5 in^3) and weight (1 oz) were facilitated by the simple construction shown in Fig. 17. The YIG spheres are biased via the magnets shown on the covers. The magnets are pressed into position when the covers are closed. The covers and unit body form a return path for the magnetic flux.

Measurements taken on the YIG FSL agree with the operating theory presented in Section I. Setup methods and measurement results are described in the following subsections.

A. Power Distributions

To determine the unit's limiting characteristics, input power, reflected power at the input, and received power at the output, are measured simultaneously (Fig. 18). The output power curve has a sharp knee at P_{in} = -8 dBm. As input power is increased above the limiting knee, output power is not as flat as it should be across the limiting range. The staircase increases are believed due to the imperfect alignment of the spheres, which results in different limiting knees. This is not a desired characteristic in a filter bank receiver.

P115-1483

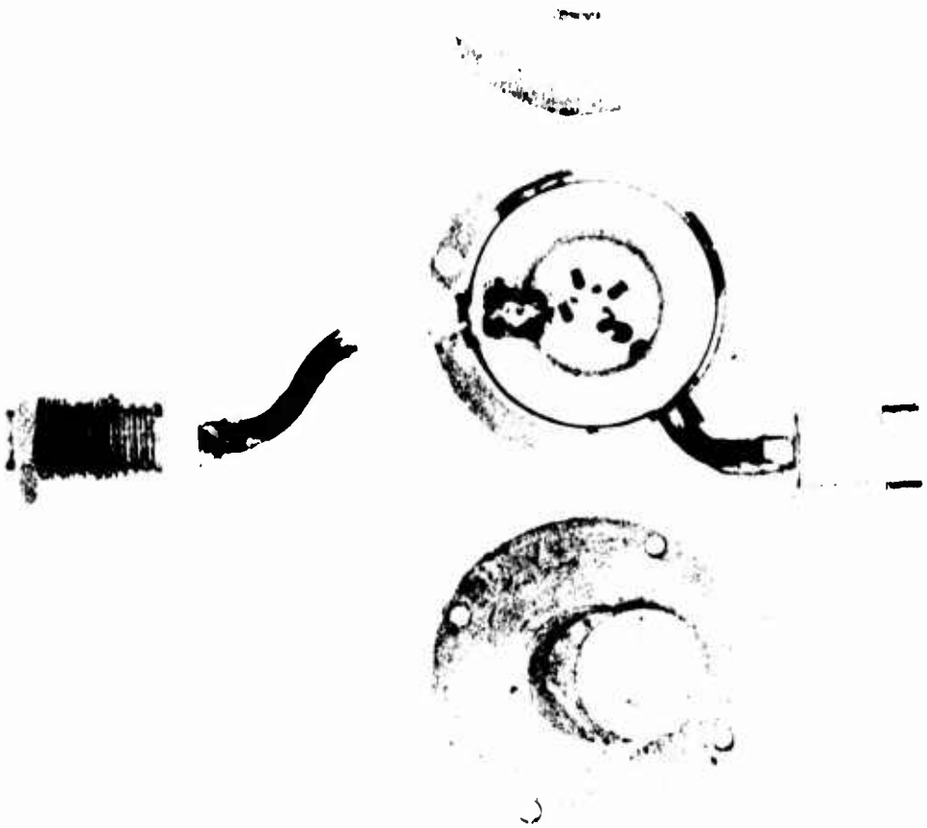

Fig. 17. A YIG FSL.

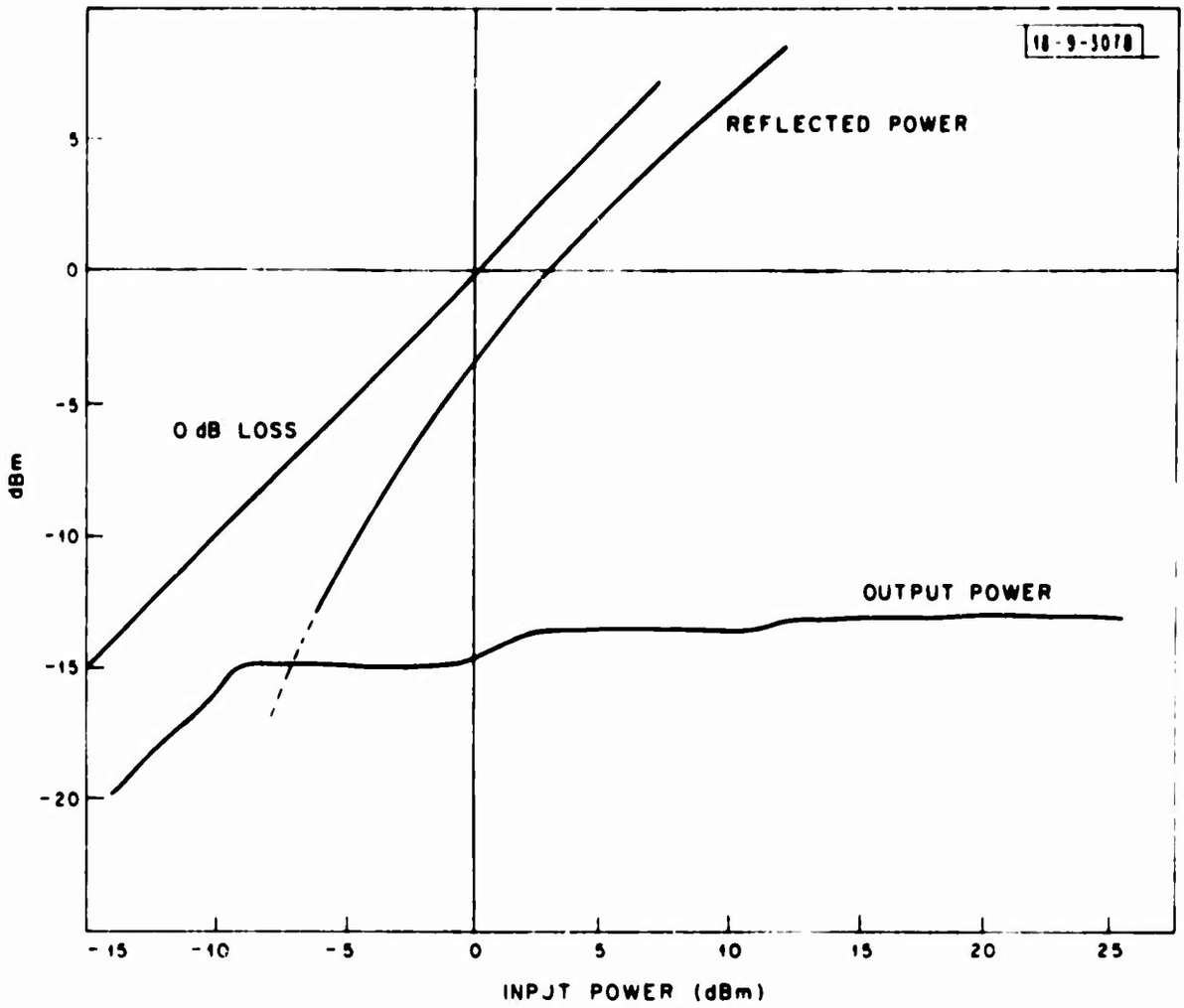

Fig. 18. YIG FSL power distribution.

It is apparent that a large amount of input power is reflected to the source by mismatch when input power is well above the limiting knee. This information verifies that the YIG FSL is a power-reflective limiter rather than an absorptive device. Heat sink and power handling capabilities within the limiting range are generally not important.

However, due to the impedance mismatch behavior, devices connected to the FSL, such as filters, no longer look into a matched load.

Two signals, both above the threshold power, were fed into the YIG FSL. Total output power was monitored by a power meter as the frequency separation was varied (Fig. 19). Output power is doubled when the two signals are separated, but when the two signals are at the same frequency, output power is reduced to the value

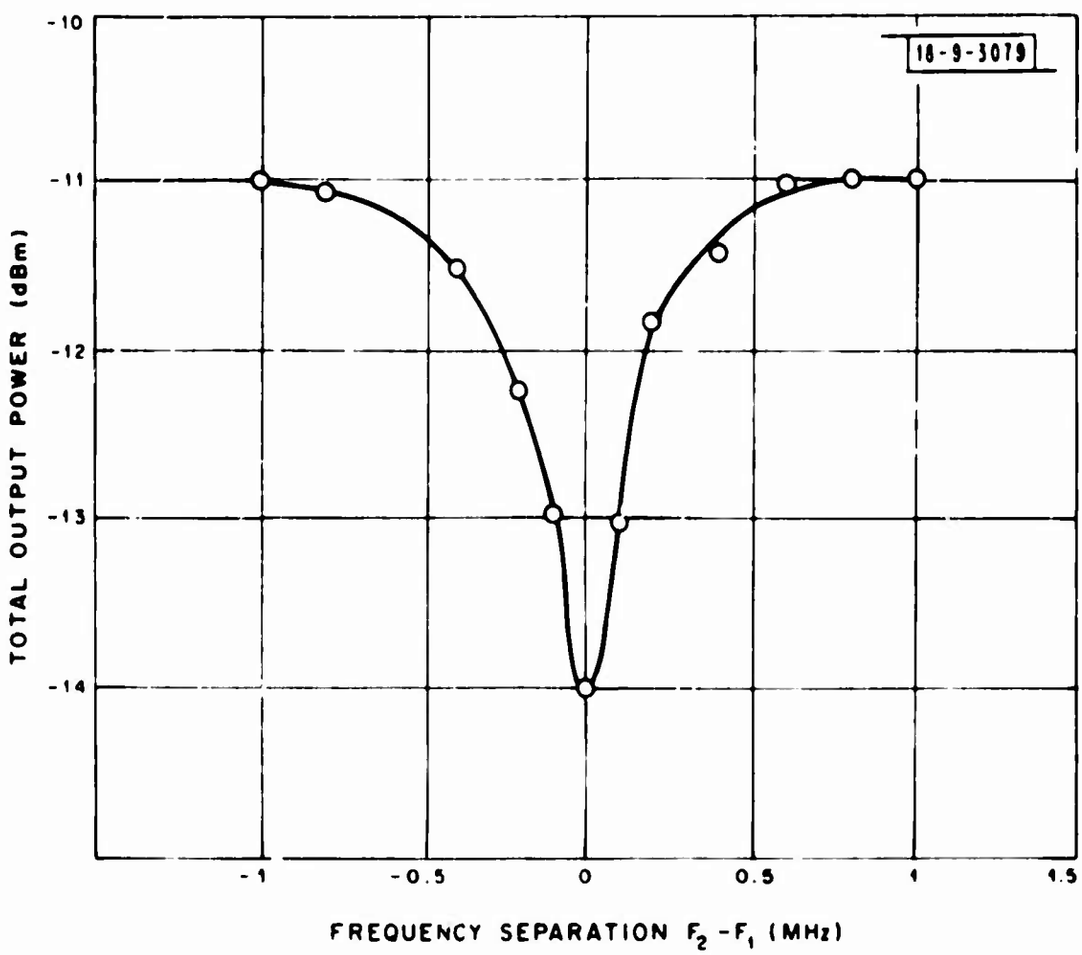

Fig. 19. Output power variation as a function of frequency separation.

when there is only one signal present. This measurement demonstrates vividly the selective limiting characteristics, and that the YIG FSL is not a constant power output limiter such as a diode clipper. In fact, the output power is n times the limited output power of a single signal when n separated signals are present.

The YIG FSL is a reciprocal device. If input and output are interchanged, a very small effect is observed. However, it could be made a nonreciprocal device[8] by different construction techniques.

B. Leakage Spike

Video waveforms were observed at the YIG FSL output when the input RF was pulse modulated. The waveforms in Fig. 20 represent input power for the following cases; on the limiting knee, +1, +3, +6 and +9 above the limiting knee, P_{th}. The waveforms in Fig. 21a are a multiple exposure of the waveforms in Fig. 20; those in Fig. 21b represent input power at 10, 15, 20, 25 and 30 dB above the limiting knee.

The details of the spike forms are somewhat limited by the pulse modulator and the detector used, but give clear indication of the relations of spike duration, amplitude, and input power . It is obvious that spike duration becomes shorter and the amplitude larger as input power is increased. Duration of the spike as a function of input is plotted in Fig. 22.

It has been reported that integrated areas under the waveforms are approximately constant.[9] However, in this measurement, the results do not follow this simple rule. The areas under the curves increased with an increase in input power (Table I).

The trailing edge spike of the YIG FSL is not observed in these measurements. In general, it has less energy and the effect is not important.

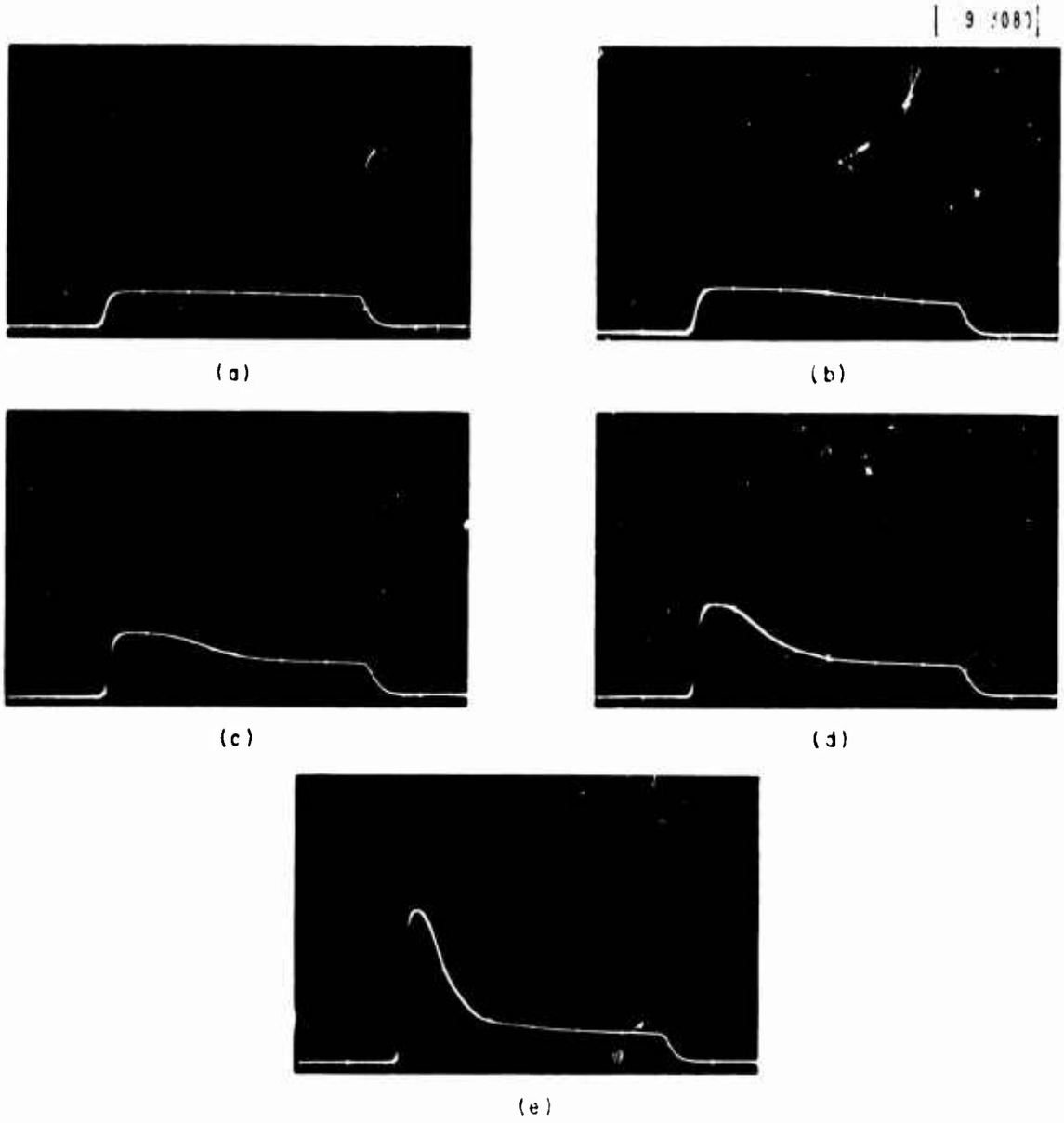

Fig. 20. Leading edge spike at various input levels. (a) 0 dB, (b) 1 dB, (c) 3 dB, (d) 6 dB, and (e) 9 dB above the limiting knee.

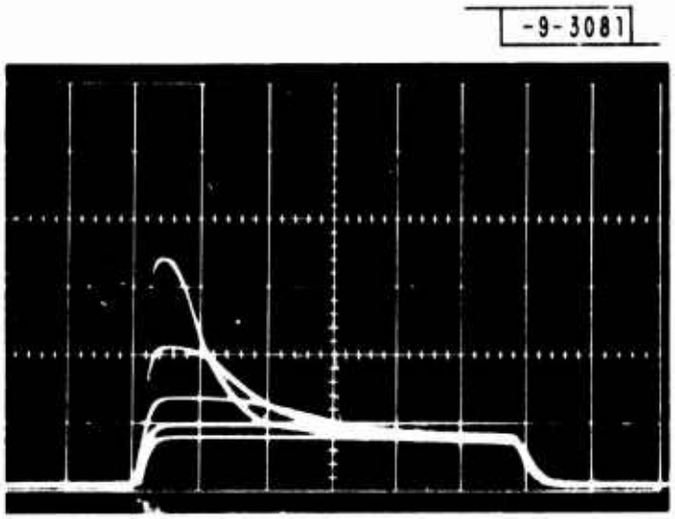

(a)

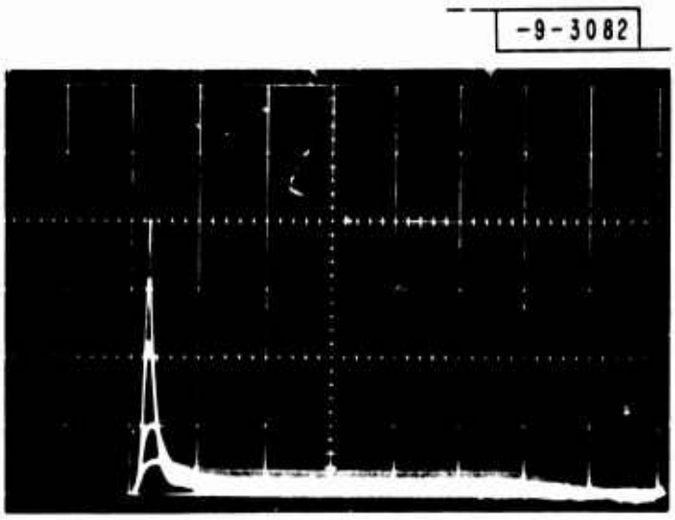

(b)

Fig. 21. a) Leakage waveforms of Fig. 20.

Fig. 21. b) Leakage waveforms corresponding to input power 10 dB, 15 dB, 20 dB, 25 dB, and 30 dB above the limiting knee.

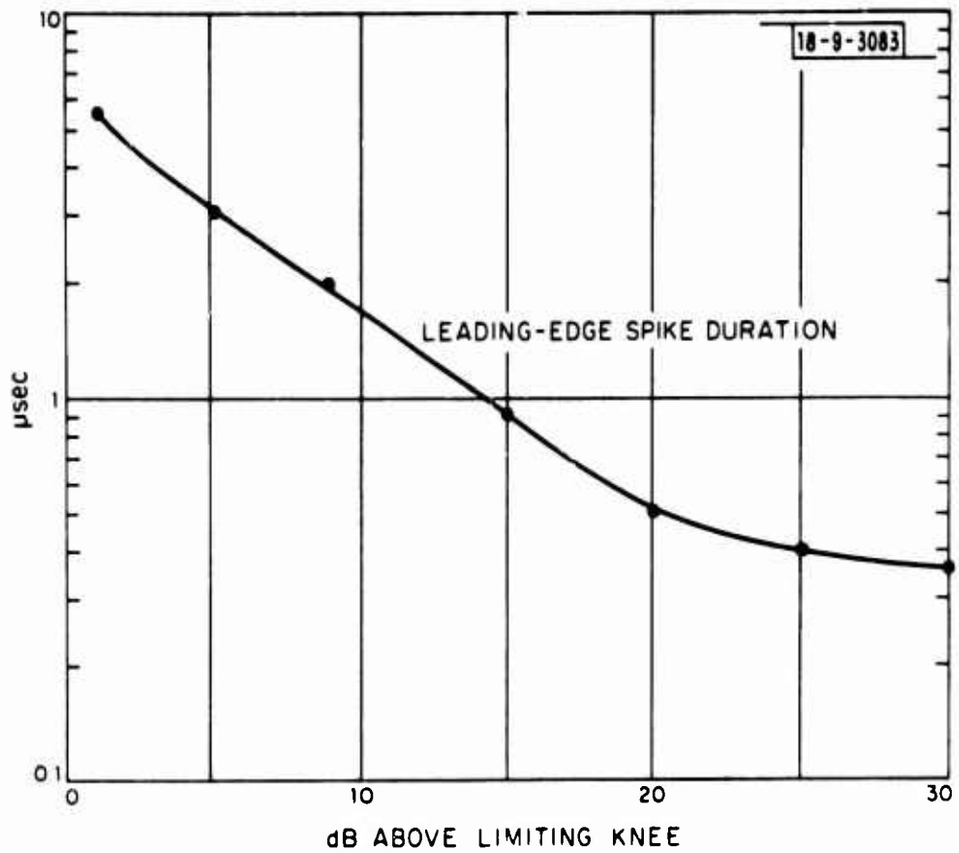

Fig. 22. Spikage Leakage duration.

Table I		
Integrated Areas Under Waveforms in Fig. 20		
Input Power (dB) Relative to P_{th}	Total Area (cm^2)	Relative Area (cm^2)
0	3.352	0
1	4.001	0.649
3	4.397	1.045
6	4.902	1.550
9	5.479	2.127

C. Small Signal Suppression

Due to the finite selectivity, $Q_{1/2'}$ of the subharmonic tanks, the small signal will be suppressed by a large limited signal. As described by the FSL model in Section I, selective limiting is degraded if two signals are separated by less than the bandwidth of the subharmonic tank.

In this measurement, a large signal well above the limiting knee was combined with a small signal just below the knee, and the two signals were fed into the YIG FSL. The level of the small signal was measured as a function of the frequency separation from the large signal at the output of the YIG FSL. The measurement was repeated as the level of the large signal was varied (Fig. 23).

It is apparent that the small signal is not only suppressed, but suppressed by a large amount if the larger signal is well above the limiting knee. It is a troublesome problem if the difference in amplitude between the signals is 40 dB or more. In this case, if a small suppression is desired so that the presence of the weak signal can be detected, the frequency separation required is a large percentage of the total operating bandwidth of the YIG FSL.

The curves in Fig. 24 are plotted from those of Fig. 23 for convenience. Each curve shows a prescribed amount of small signal suppression in dB. For a given small signal suppression, as the large signal power is increased, greater frequency separation is needed. Thus, the bandwidth at the -3 dB suppression points, for example, is a function of the limited large signal amplitude.

To investigate the small signal suppression at a very small frequency separation, Kotzebue[7] performed the measurement by square-wave modulating the small signal

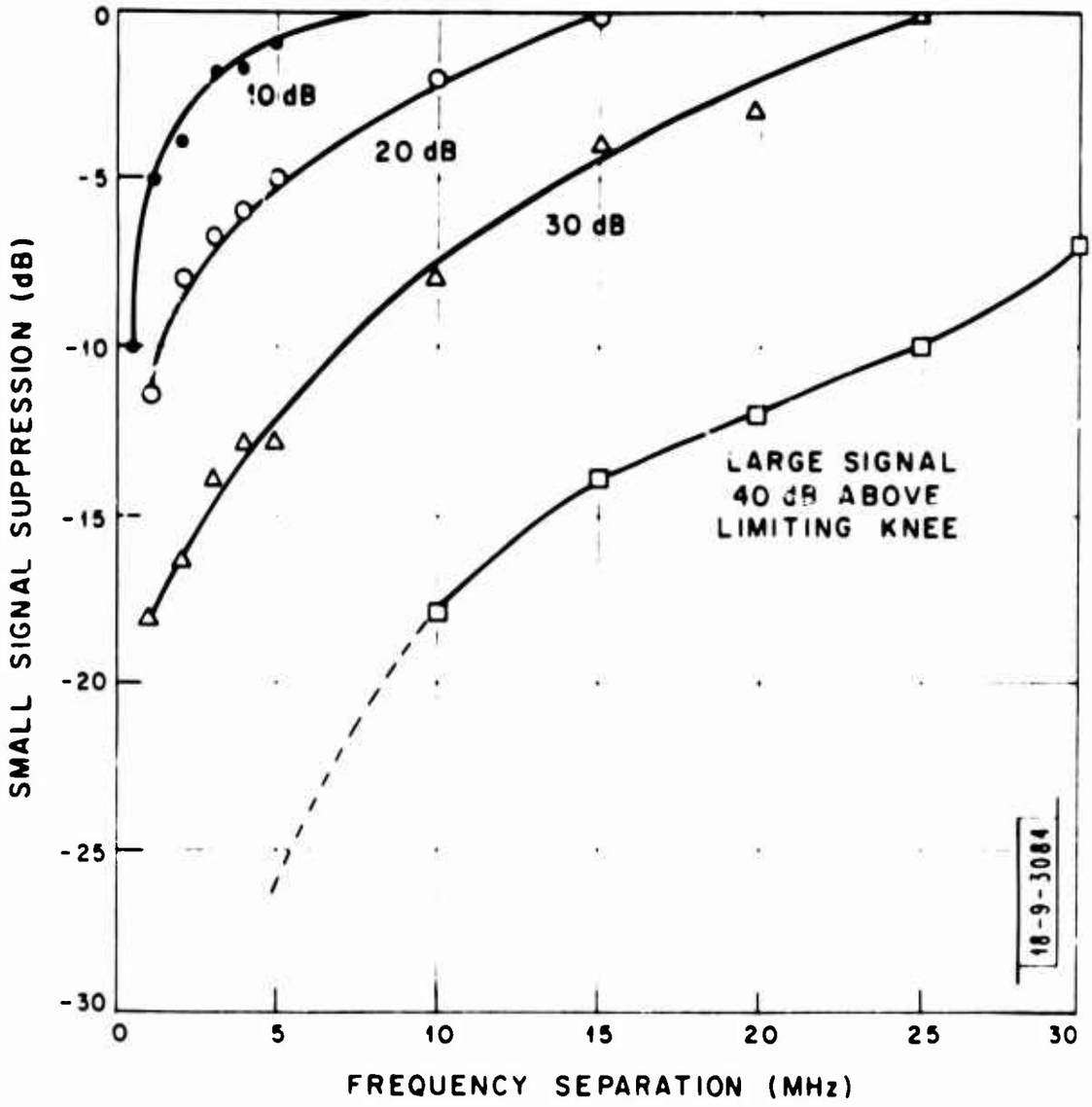

Fig. 23. Small signal suppression of two signals.

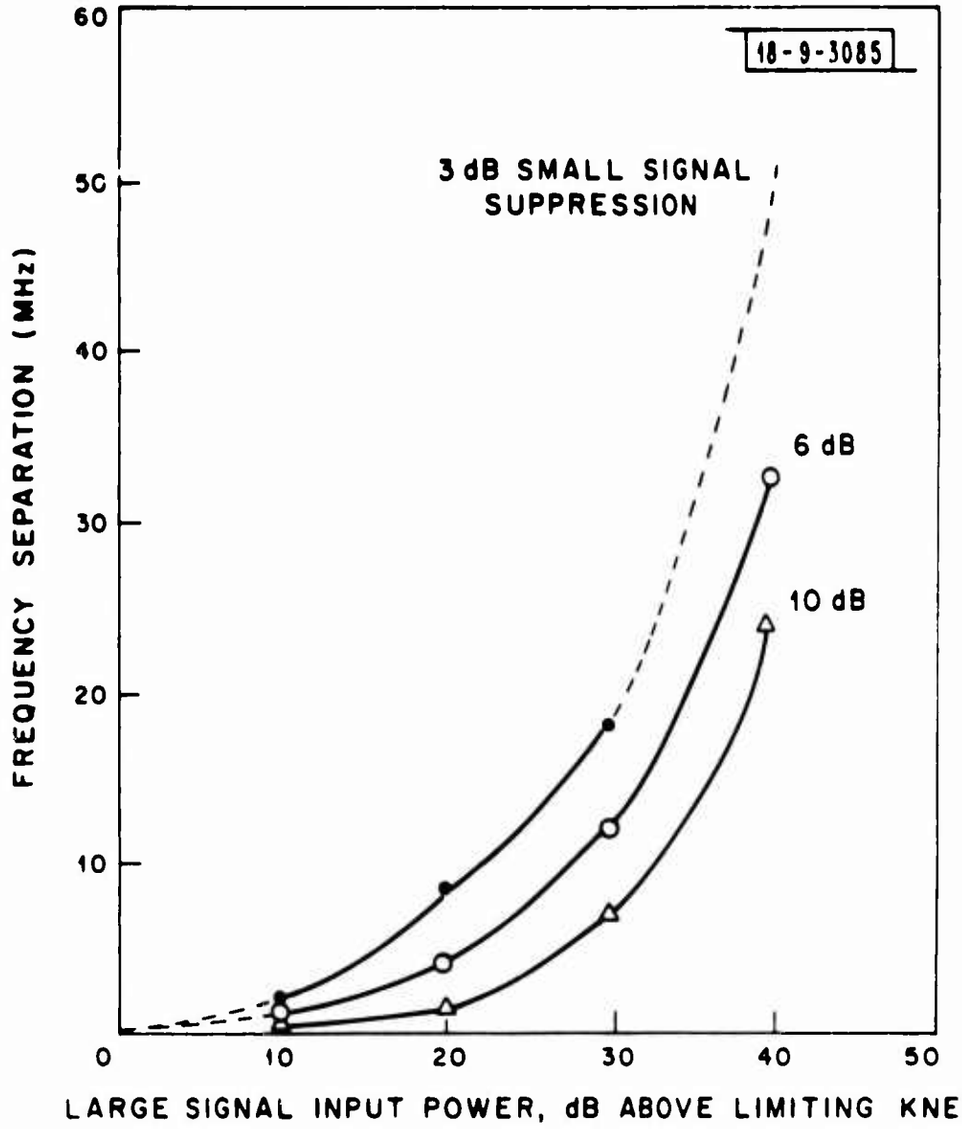

Fig. 24. Frequency separation required as a function of large signal strength for a given small signal suppression.

at input (Fig. 25). The amplitude of the modulated signal was then observed at the output. The device was tested at a frequency 2700 MHz which is higher than that of the YIG FSL used in this measurement.

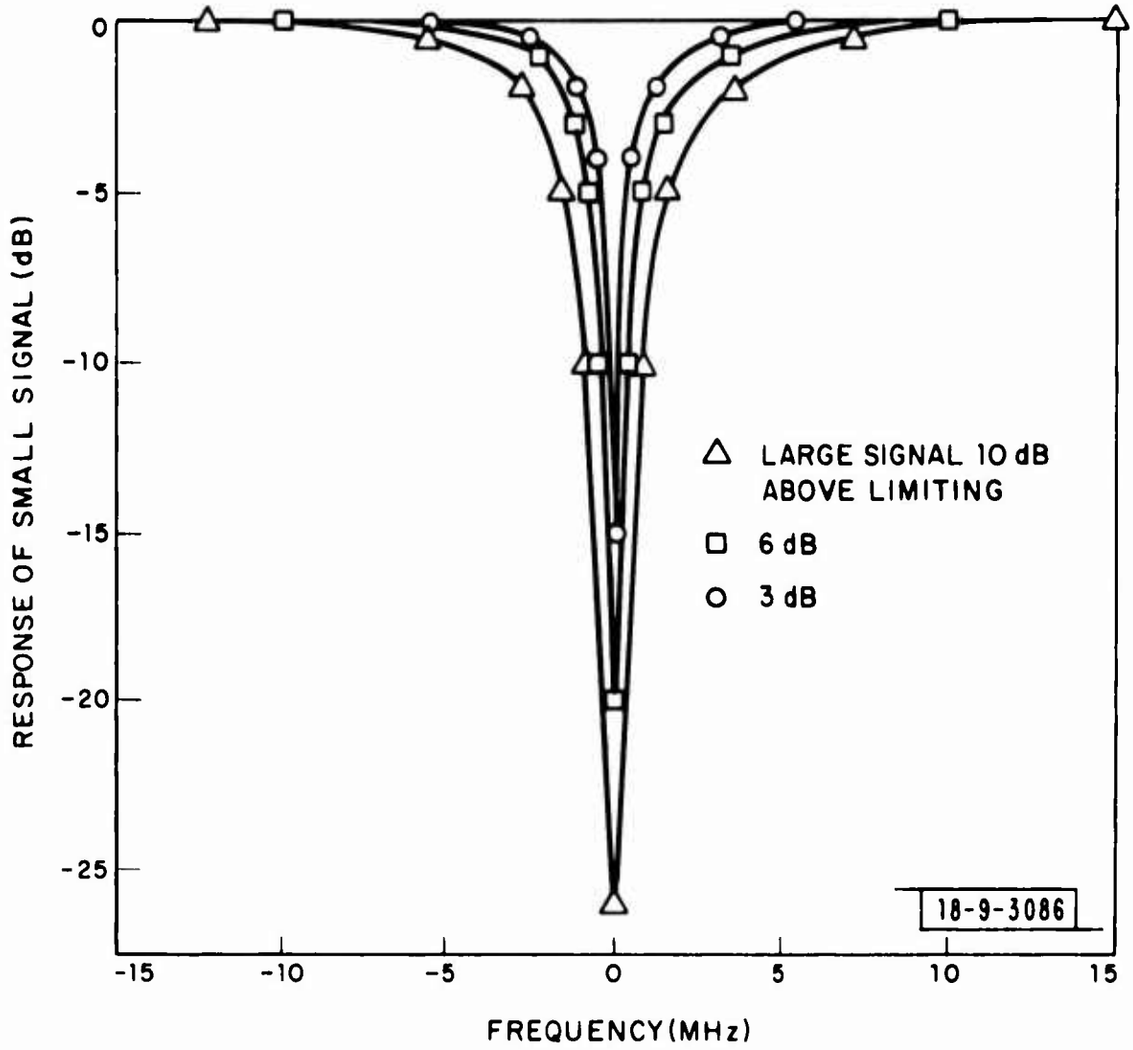

Fig. 25. Small signal suppression at 2700 MHz as a function of frequency difference and large signal power level. (after K. L. Kotzebue)

D. Intermodulation Products

To investigate 3rd order IM products, two equally powered CW signals were combined by matched coupler, fed into the YIG FSL, and monitored by a spectrum analyzer.

There was some doubt about the 2nd order IM-type products that were generated.

However, the spectrum was clean at frequencies outside the operating band. The only products observed were those whose frequency $F_{IM} = |m|f_1 + |n|f_2$ falls in the unit's operation frequency band.

3rd order products $2f_1 - f_2$ and $2f_2 - f_1$ were the strongest products observed with much higher amplitudes than other higher order products.

There is no simple way to characterize the IM products such as "cross modulation" or "intercept point" methods used in amplifiers. Since the YIG FSL is a frequency-selective device, the IM products are a function of the amplitude as well as frequency spacing.

For frequency separation of the order of 1 MHz and powers above the limiting knee, the device generates strong 3rd order IM products (Figs. 26 and 27). These products are greatly reduced as frequency separation is increased.

As the frequency separation decreases, the 3rd order IM product levels tend to approach a level some 3 dB or so below the fundamental output level. When two signals are extremely close in frequency, measurements are limited by the stability of the signal generators and the resolution of the spectrum analyzer.

Higher order products (5th and 7th order) are also noticeable though small in magnitude. The magnitudes of 3rd, 5th and 7th order products in two equal amplitude signals 20 dB above the limiting knee were compared (Fig. 28).

E. Linear FM Responses

An RF generator with a sweep rate much higher than the order of 1 MHz per μsec is required to investigate limiting characteristics when a linear FM signal is applied. As such a high sweep rate is not generally available in a conventional sweep generator, a special setup was provided by Mr. G. T. Flynn and Mr. A. J. Yakutis of the R. F. Systems Group; an S-band voltage-tuned

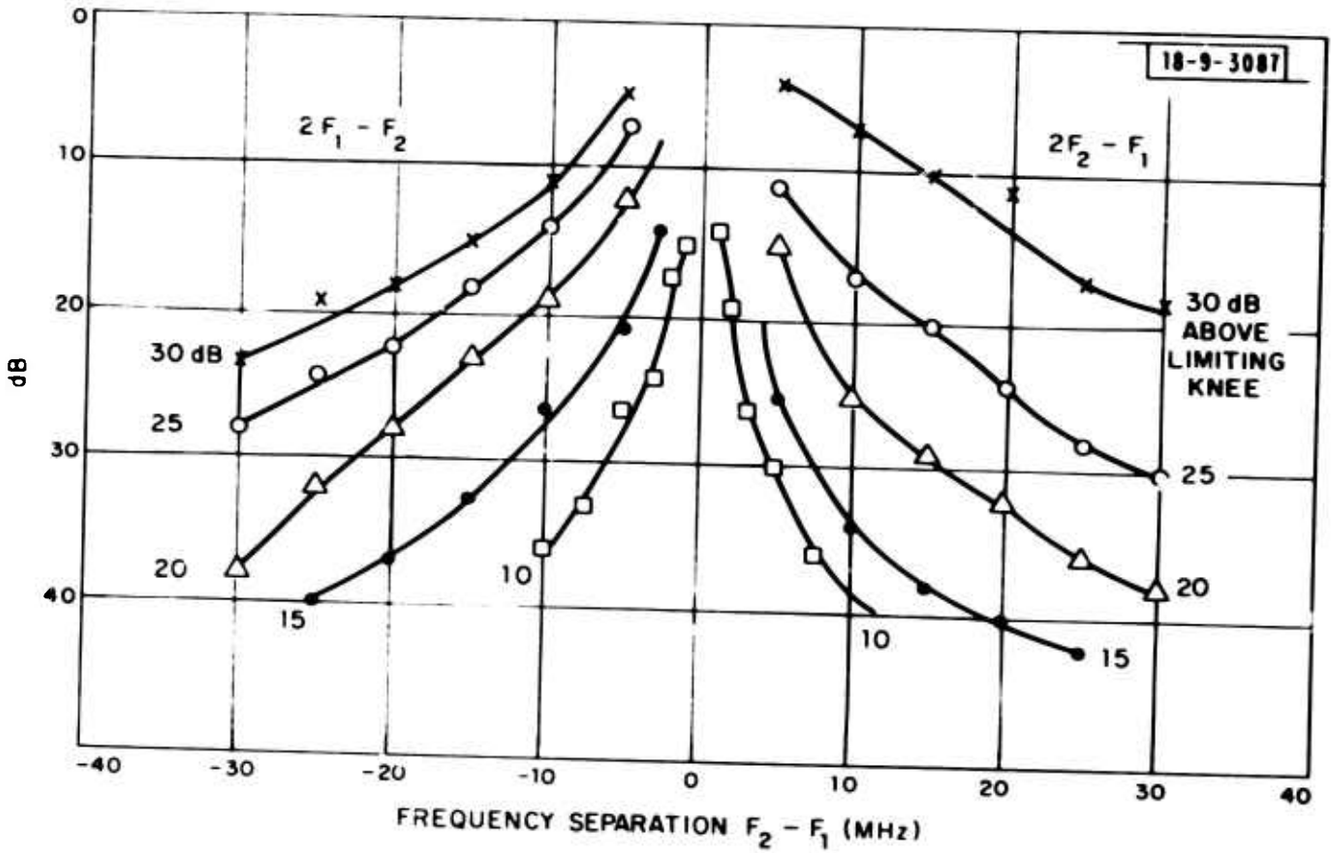

Fig. 26. YIG FSL 3rd order intermodulation products level versus frequency separation for two equal amplitude signals.

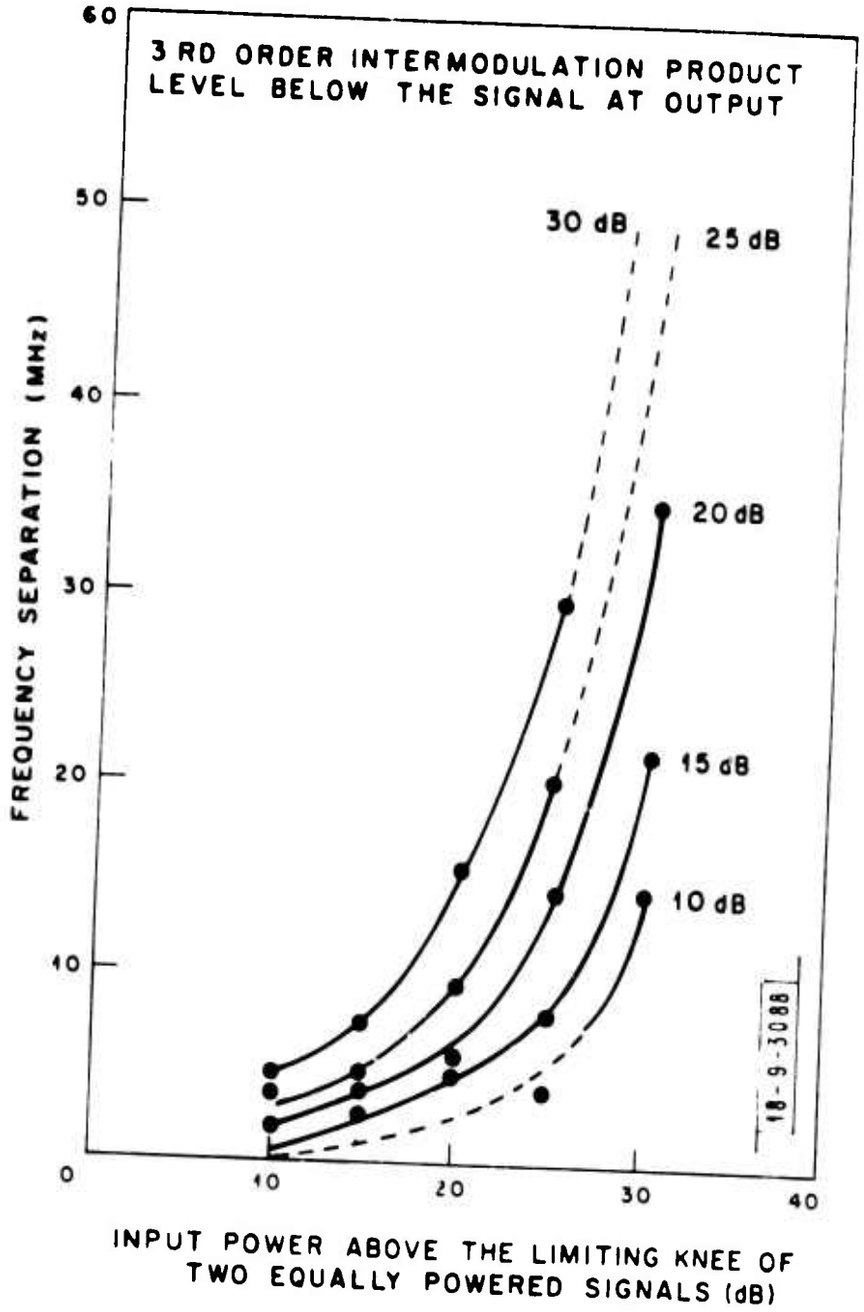

Fig. 27. Frequency separation required as a function of two equally powered signal levels for prescribed 3rd order IM products.

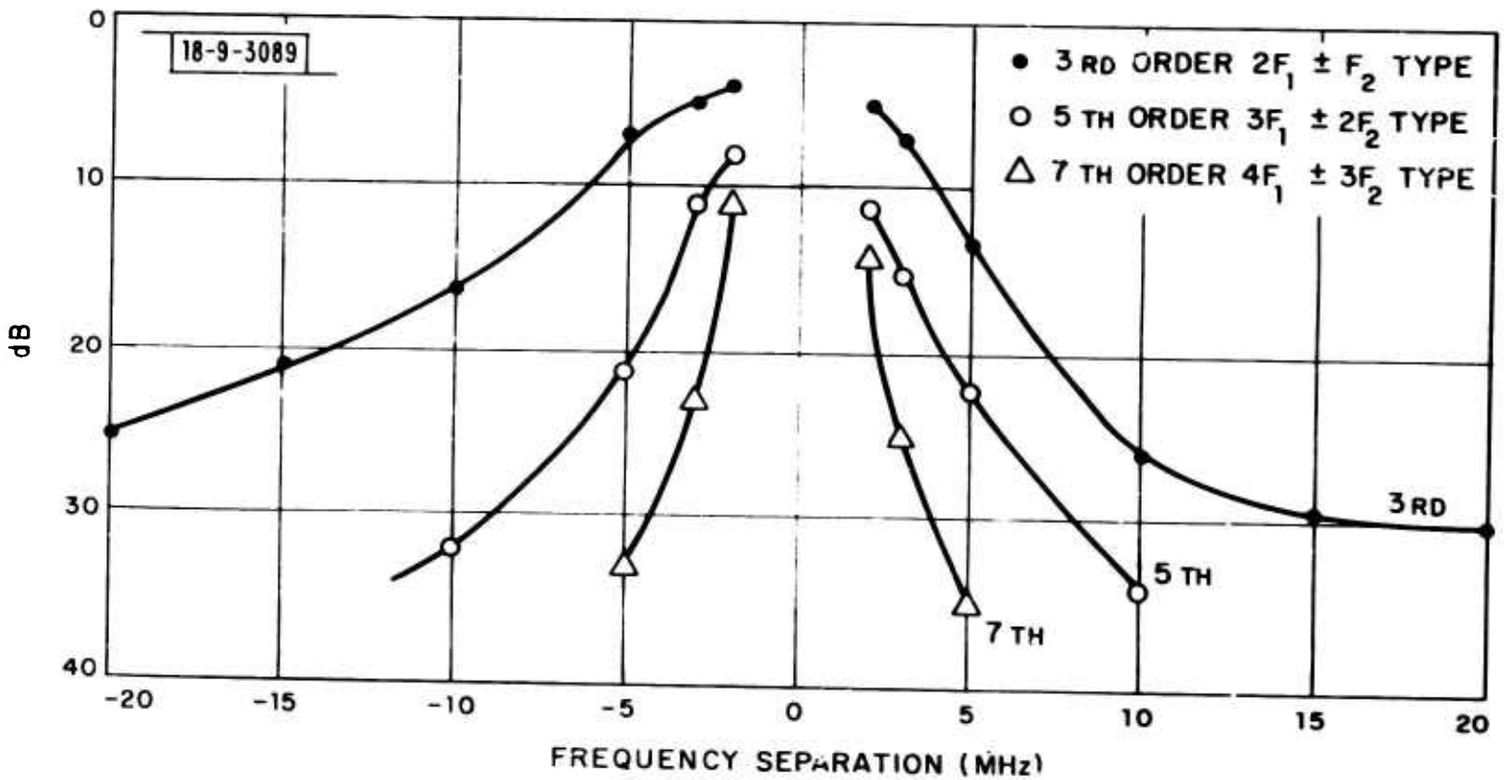

Fig. 28. YIG FSL intermodulation products at output when two equal-powered signals 20 dB above the knee are fed into input.

magnetron (VTM). Linear frequency modulation (LFM) was achieved by a linear sawtooth generator in series with the cathode and its high voltage power supply. By varying the amplitude of the sawtooth voltage or the repetition rate, the setup provided an extremely fast sweep over a wide frequency range. The signal was then used as an LFM source fed into the YIG FSL.

In this measurement, the sawtooth voltage amplitude was fixed so that the RF frequency had the same start and stop frequency for various conditions (Fig. 29).

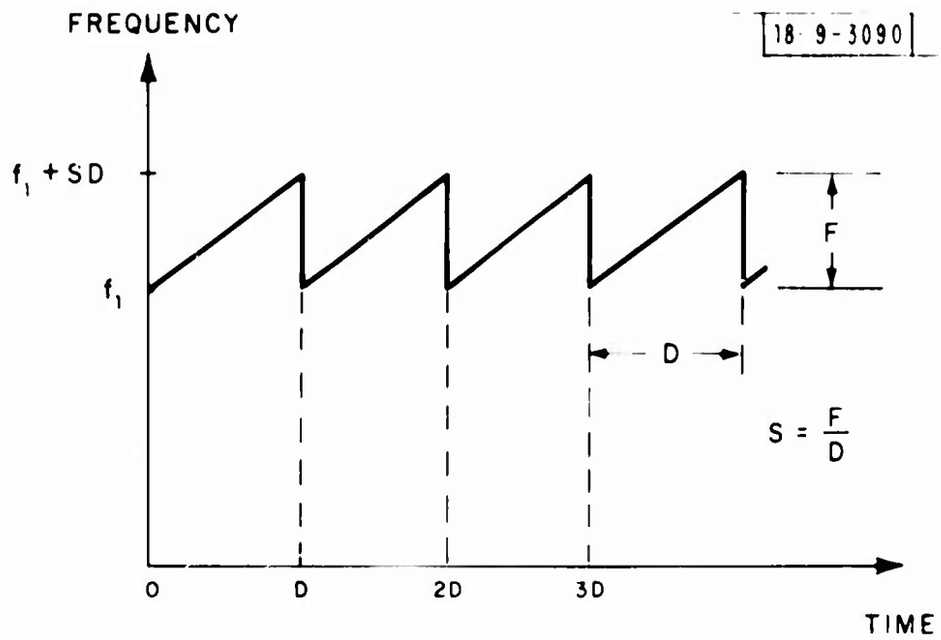

Fig. 29. Sawtooth-varying frequency.

The sweep rate S-MHz/μsec was varied by changing the repetition rate of the sawtooth generator. The purpose of such an arrangement was to operate the unit in the same portion of the frequency band for different conditions and ensure that this was within the operating band of the unit.

Output power plotted as a function of input power for different sweep rates (Fig. 30) shows clearly that as sweep rate increases, the limiting threshold power also

increases. Once the threshold power is reached, the output power is kept constant in the same manner as a fixed frequency signal.

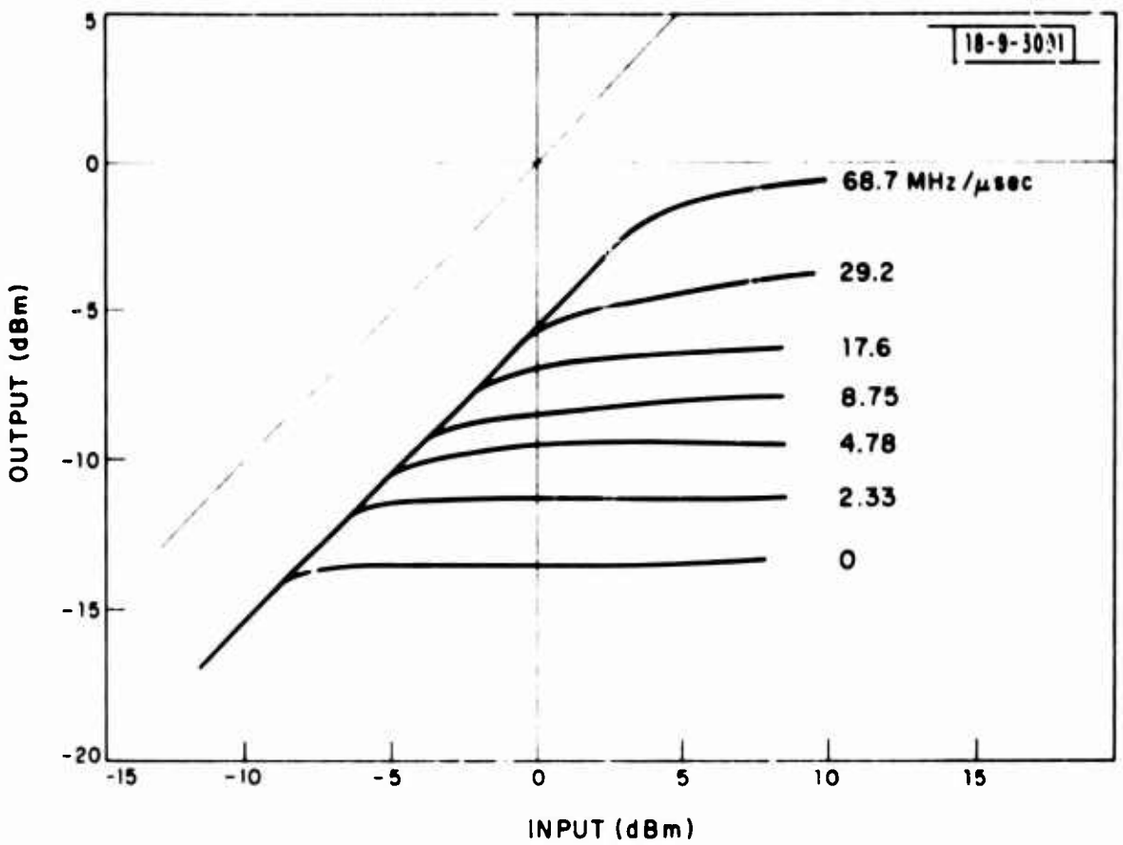

Fig. 30. Limiting characteristics versus linear FM signal.

A soft limiting knee tends to appear at an extremely high sweep rate when output power is not constant. The exact reason for this is not known at this time. However, at an extremely fast sweep rate, the flyback time duration of the sawtooth generator becomes appreciable compared to the total duration. It is believed that subharmonic oscillation in the $\omega/2$ tank then is composed of two factors: one occurring during the sweep; the other contributed by all the previous forward and flyback sweeps. The influence of these factors on the limiting characteristics have to be considered.

III. Application of the YIG FSL to Filter Bank Receivers

A. YIG FSL as a Level Normalizer

Since the YIG FSL is a self-adaptive limiter, signals of different levels are attenuated individually by the FSL according to their strength. Ideally, all signals will have the same amplitude at the output if the signal levels fall within the limiting range. The signals, therefore, are normalized to the output limiting level of the YIG FSL and are fed into the filter bank. Thus, exotic design of the filter bank can be avoided and size and weight can be minimized.

However, due to the finite selectivity, $Q_{1/2}$, of the FSL, small signals will be suppressed by the limited large signals when two signals are separated by only a small amount. Therefore, output levels are not the same where signals are spaced closely together or are widely divergent.

The extent of normalization can be determined by comparing the difference in levels at the input with that at the output of the FSL. The curves in Fig. 31 are plotted by using the data in Fig. 23 for two input signals, one on the limiting knee and the other above the knee. The difference in dB at the input is projected to the difference at the output for a prescribed frequency separation, Δf in MHz. The zero gain line indicates no normalization by the YIG FSL. Points below the zero gain line show that the level difference at the output is less than at the input: normalization gained. Points above the zero gain line show a loss or denormalization.

The successive lines indicate that as frequency separation is reduced, the curves tend to approach the zero gain line. In essence, normalization gain is reduced by the fact that small signal suppression increases progressively as the frequencies approach each other.

When the signals approach zero separation, all curves coincided with the line $\Delta f = 0$, the case for hard limiting.

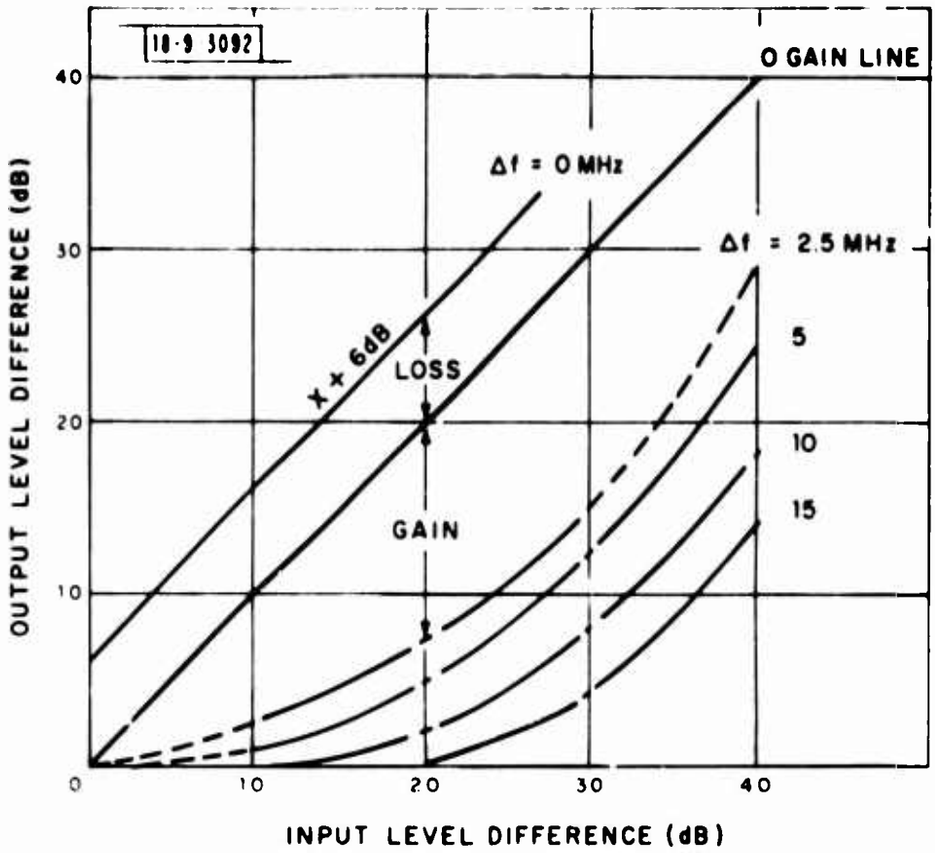

Fig. 31. YIG FSL normalization gain (curves plotted from data in Fig. 23 - small signal suppression).

Obviously, operating conditions above the zero gain line should be avoided. However, in the real environment, one has no control of frequency separation and the strength of received signals. Nevertheless, the conditions represent very close frequency spacing -- of the order of 1 MHz -- which is generally closer than the bandwidth for filter banks considered to date. Normalization of frequencies separated by less than 1 MHz is basically limited by the large dynamic signal range.

YIG FSL's can be cascaded in series if each stage can be isolated. By properly adjusting threshold levels, larger normalization gain than with a single FSL can be achieved. This hypothesis is explained in the next subsections.

B. Cascading YIG FSL's to Achieve Large Limiting Range

One problem with a YIG FSL is its relatively short limiting range compared with the dynamic range of signals that are encountered in the environment. To normalize a given range of signals, an FSL needs a limiting range that at least equals the signal dynamic range. YIG FSL's with a limiting range of 20 to 25 dB are easily obtainable by using a single sphere. The multi-sphere technique permits one to achieve a larger limiting range, closer to the requirement. However, due to interactions of the spheres, the range is still basically limited.

Two other effects can influence YIG FSL design at very large input power: heat and nonlinear mode of the YIG FSL, which are also part of the difficulties in achieving large limiting range.

Although the YIG FSL is generally a power reflective type device, at extremely large input power, the absorbed power causes higher sphere temperature. The heating effect could lower its magnetization and thereby raise the level of the limiting knee. Consequently, output power cannot be kept at a constant level.

The YIG sphere will enter a premature decline nonlinear mode at a certain high power level. The premature decline mode is a 2nd order nonlinear effect that uses the

spin-waves of the same frequency as the input frequency. Whereas, the coincidence mode, being the 1st order nonlinear effect, uses the spin-waves of half the input frequency. The frequency-selective characteristic of the YIG limiter has only been observed at the coincident mode depicted by the FSL mode in Section I.

Another way to achieve a large limiting range is by cascading FSL's and amplifiers, alternatively. By properly adjusting the gain of the amplifiers, the total limiting range could be the sum of the individual ranges.

The system in Fig. 32a shows that two identical FSL's, each with a 20-dB limiting range. The attenuator sets the first FSL to a higher limiting range, and the amplifier sets the second FSL on a lower limiting knee. The result: the end of the second FSL range is the beginning of the first. The amplitude normalization process of three hypothetical signals at various points in the system is shown in Fig. 32b. The FSL's are not exposed to excessive high power levels due to the attenuator. The limitations of heat effect and premature decline mode can then be avoided. Small limiting range FSL's and compact RF amplifiers will be used to investigate the feasibility of this hypothesis.

C. 3rd Order IM Products to Filter Bank Receiver

The presence of 3rd order products represents a false signal since it is generated by the YIG FSL. Although it has a more significant amplitude than higher order products, the amplitude is below the fundamentals at the output. Therefore, in a filter bank receiver, 3rd order products are less bothersome if the threshold of the triggering circuit is set above the level of the 3rd order products.

The data in Fig. 26 have been plotted in a different way as shown in Fig. 33 to show the relation of fundamentals and 3rd order products. Compare the output levels; fundamental signals F_1 and F_2 are at a much higher level than $2F_1 - F_2$ for most of the limiting range. As power is increased or frequency separation drops below

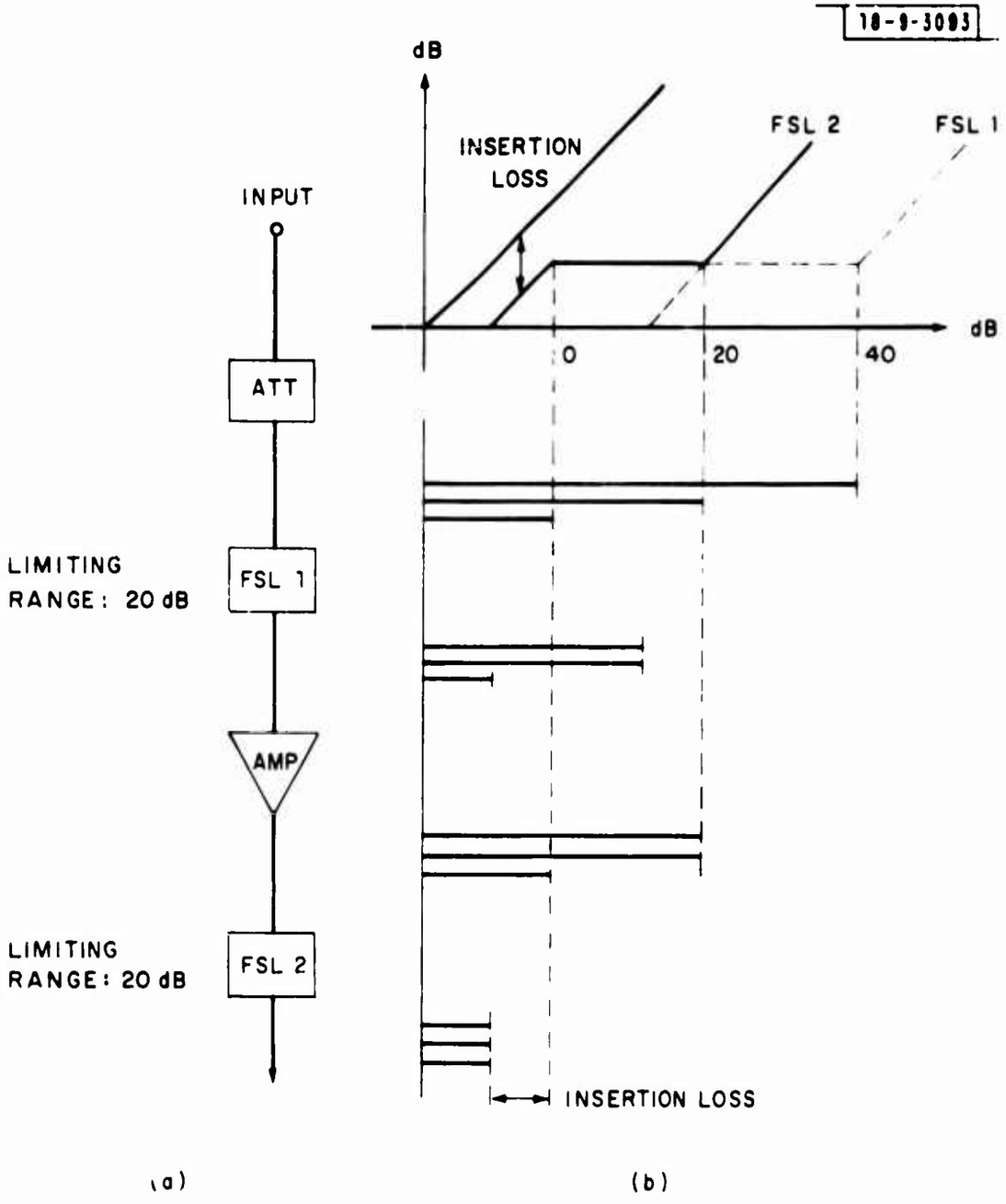

Fig. 32. Cascade FSL's to achieve large limiting range.

1 MHz, the 3rd order tends to approach a level just 3 dB below the fundamental level (Section II D). Therefore, most of the detrimental effect caused by 3rd order products can be overcome by setting the triggering level just 3 dB below the level of the fundamental signals. The false signal can then be ignored.

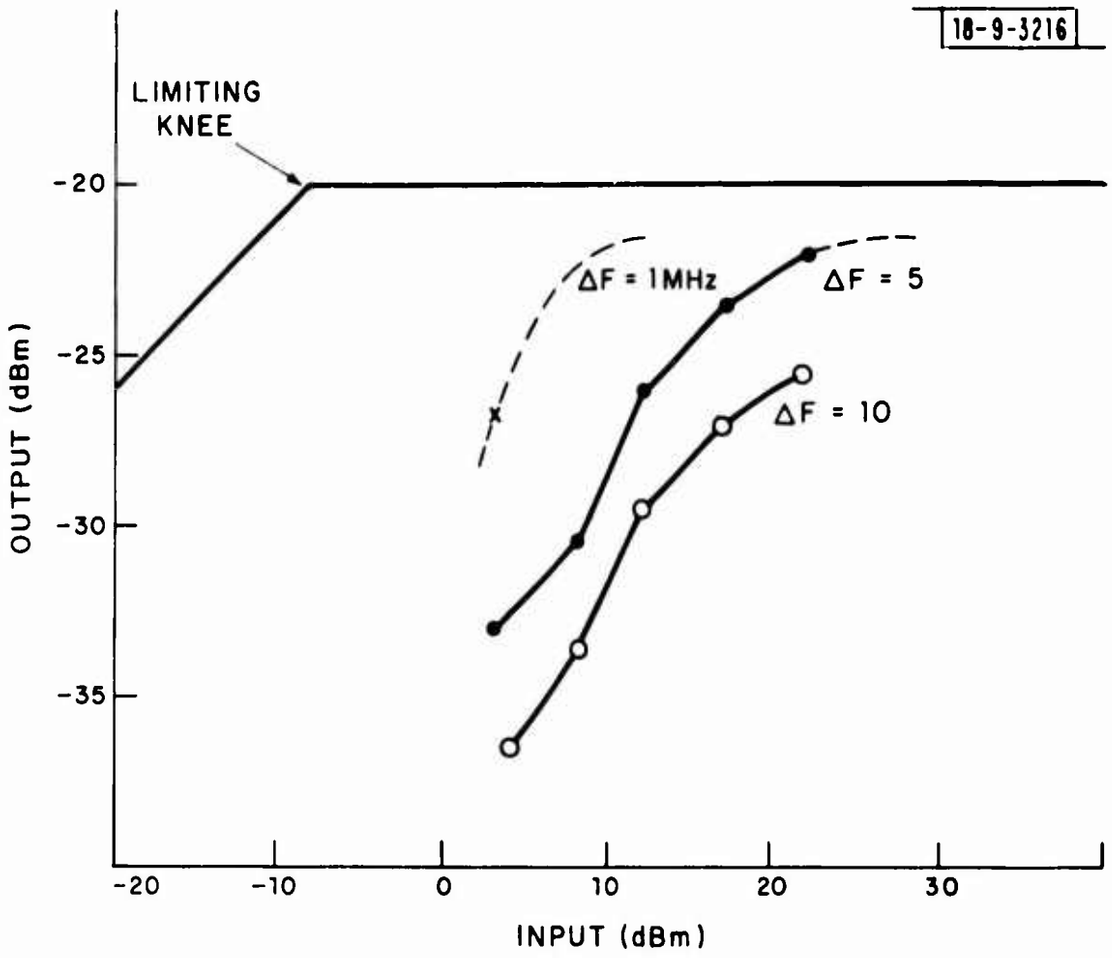

Fig. 33. Fundamentals and 3rd order products.

D. Small Signal Suppression and the Threshold Level Detector

The small signal suppression by a larger limited signal in a YIG FSL could be a serious problem. When the threshold detector at the output of the filter is preset at a fixed level, the small signal may not be detected -- a catastrophic defect for a filter bank receiver under worst-case conditions.

An obvious way to regain the suppressed small signal is to deliberately set a lower threshold triggering level, for example, at -6 or -10 dB instead of at -3 dB bandwidth point depending on the dynamic range of the signals (Fig. 34). The penalties in doing so are that the ambiguous areas are increased, resolution of the filter bank reduced. Moreover, at the worst-condition when two equally large signals are received, their 3rd order products, as aforementioned, can reach a level only 3 dB below the fundamental, could trigger the threshold detector and record a false signal. However, these penalties are at most a reduction in efficiency of the system rather than complete loss of the signal.

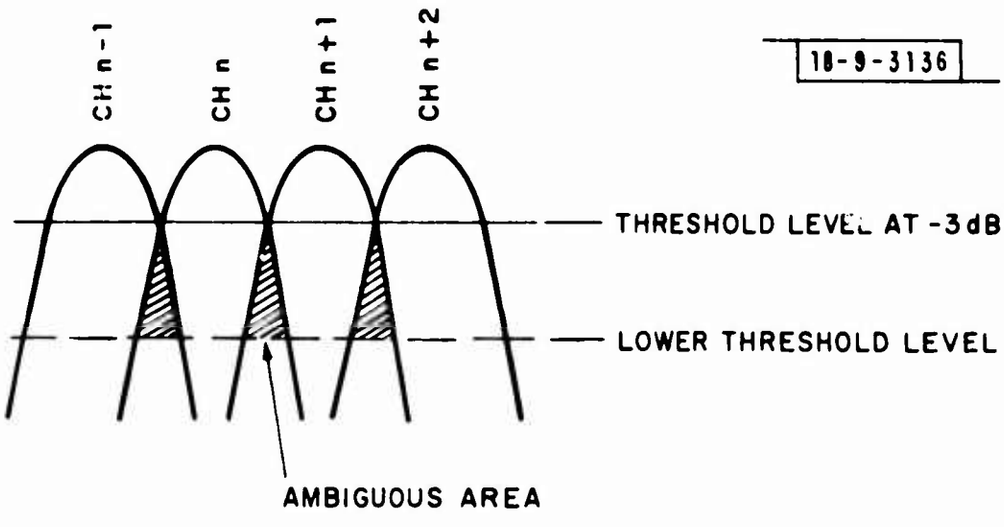

Fig. 34. Trigger level and ambiguous area.

Consider the problem of a threshold level detector that under worst-case conditions is not triggered by 3rd order IM products but by the suppressed small signal as well as by the large signal. In a given dynamic range of signals, the design can be met with certain frequency separation.

Worst-case conditions for keeping the detection from being triggered by 3rd order products exist when two equal peak power signals are received (Fig. 35). Worst-case conditions that ensure the smallest signal trigger will exist when received together with a peak signal (see Fig. 35). These curves intersect at a point corresponding to frequency separation F_s and normalized signal level N_L.

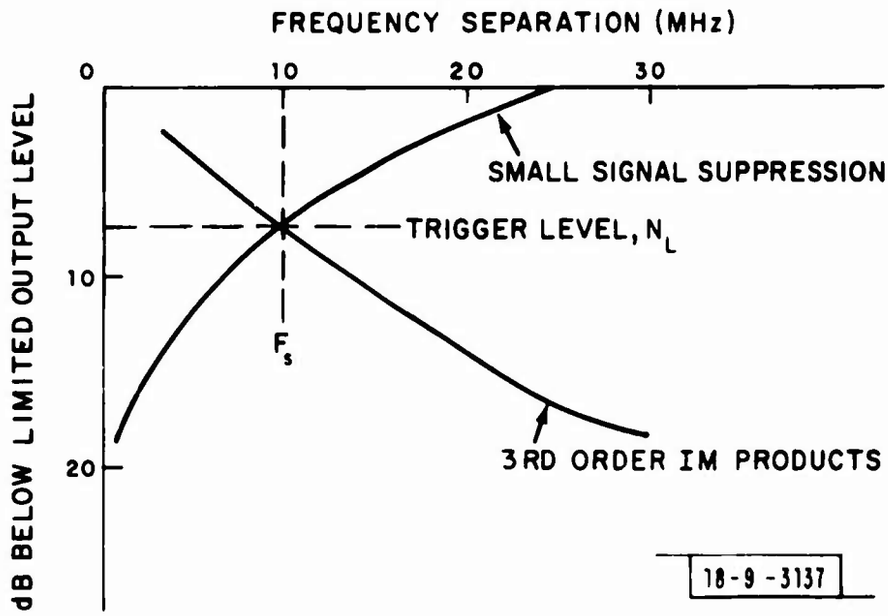

Fig. 35. Worst-case conditions and threshold level.

If the trigger level is set at level N_L, the signals with frequency separation larger than the F_s will trigger properly since 3rd order IM products are below the trigger level and the suppressed small signal is still above the trigger level. Whereas, signal spacing is less than the required separation, F_s, small signals are not

detected and the 3rd order IM products are not kept from the trigger. Consequently, the minimum frequency separation is defined by the worst-case condition when the signal dynamic range is given. As expected, the larger the dynamic range, the greater the separation, F_s, required.

One is forced to set a low trigger level when considering worst-case conditions, therefore, the ambiguous area is increased, or a better filter roll-off rate must be obtained.

E. Response of a YIG FSL and Filter Bank Receiver to an LFM Signal

A row of contiguous subharmonic tanks connected to an ω tank, and a column of filter banks connected at the output of the ω tank through the amplifier represents a YIG FSL and filter bank receiver (Fig. 36). An amplifier provides some isolation.

The response of the YIG FSL to an LFM signal has been analyzed and measured (Section II 4). As mentioned, the effective signal level to the subharmonic tank is reduced due to the sweeping effect. The result is that the limiting knee and output level of the YIG FSL is higher (see Fig. 30).

The response of a bandpass filter to a sweep signal is well known and sometimes described as the gliding effect.[10] Basically, the signal sweeps over a large number of channels in sequential fashion. The filter response depends on the sweep rate.

At a very low sweep rate, the filter output is simply a plot of its frequency response. However, at an extremely high rate, the LFM input signal appears as an impulse signal. The output approaches the impulse response of the filter. The response between these extremes is a function of the sweep rate and the shape of the bandpass filter. Nevertheless, the output of the bandpass filter to an LFM signal is a pulse waveform in the time domain, and the amplitude depends on the rate of sweeping.

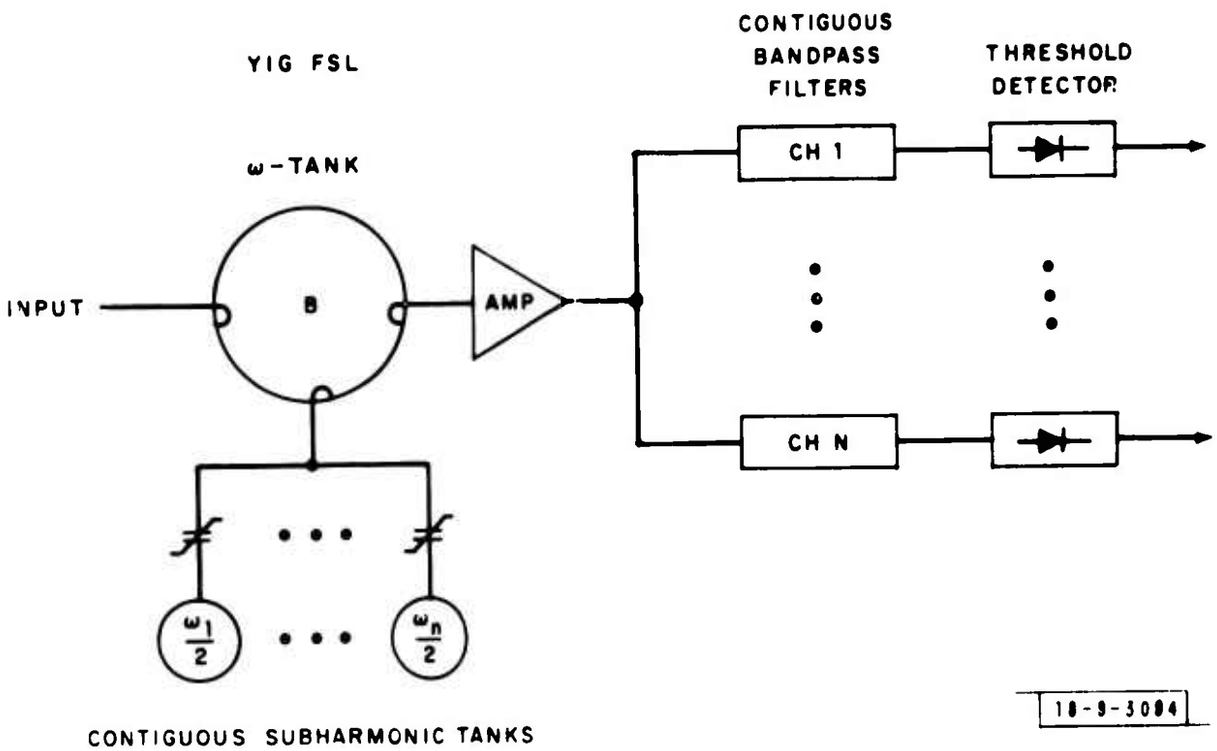

Fig. 36. YIG FSL and filter bank receiver.

A signal with sweep rate s (Hz/sec) can be represented by

$$f(t) = \exp\left[j\pi st^2\right].$$

If f(t) is applied to a Gaussian-shaped bandpass filter,

$$H(\omega) = \exp\left[-1/2\left(\frac{\omega}{\sigma}\right)^2\right].$$

The response at the output of the filter would be [11]

$$z(t) = \frac{1}{\left[1+\left(\frac{2\pi s}{\sigma^2}\right)^2\right]^{1/4}} \exp\left[-\frac{\frac{\sigma^2 t^2}{2}}{1+\left(\frac{\sigma^2}{2\pi S}\right)^2}\right]$$

where $\sigma = \pi \Delta f / \sqrt{\ln 2}$.

The amplitude of $|z(t)|$ can be plotted as a function of sweep rates when the bandwidth of the Gaussian filter is given. One such curve of $|z(t)|$ is plotted in dB versus MHz/μsec (Fig. 37). In general, for a given bandpass filter, the faster the sweep rate, the lower the output amplitude. Therefore, above a certain sweep rate, without some means of compensation, the amplitude could be reduced to below the threshold level of the triggering circuit. Consequently, no signals are detected and identified.

The response of the YIG FSL to the LFM signal has an opposite effect from that of the bandpass filter described. For a system like the one shown in Fig. 36, an increase in amplitude at the YIG FSL output will offset amplitude reduction from the bandpass filter. When a sweep signal is applied, the net change could be cancelled at the output; the identification capability, therefore, is not degraded.

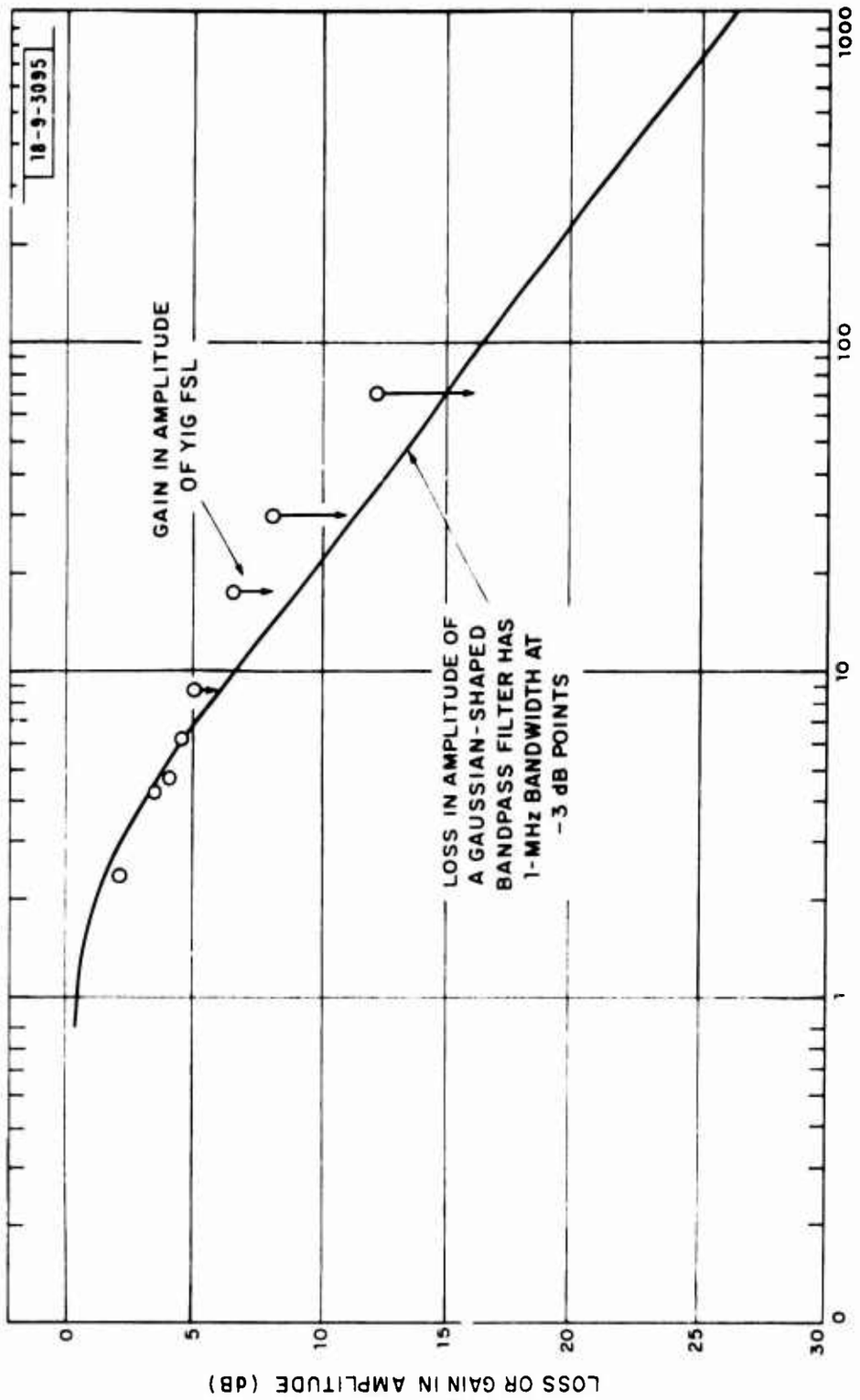

Fig. 37. Comparison of amplitude variations of YIG FSL to a Gaussian bandpass filter.

A comparison of the loss at the ouput of a 1-MHz bandpass filter with the gain by the YIG FSL as a function of sweep rate is given in Fig. 3'. The offset is excellent up to a sweep rate of about 10 MHz/μsec. At higher rates, the measured output level of the YIG FSL is not at a constant value (Section II E) but the offset is still good. It seems reasonable to say that the YIG FSL can be used advantageously in a filter bank receiver to detect linear frequency modulated signals.

IV. Conclusion

A basic parametric FSL model was used to predict the characteristics of a YIG FSL under different signal forms and signals existing simultaneously. The predictions agreed qualitatively with the experimental results.

Experimental data obtained from a procured YIG FSL should typify all YIG FSL's designed with power and selectivity characteristics scaled to the value of this unit.

A way to achieve a large limiting range by cascading the YIG FSL's and amplifiers is proposed. This method is an alternative to using YIG spheres alone, which has proven difficult to perfect.

The YIG FSL has the property of raising output level when an LFM signal is applied, which is desirable for frequency identification and detection in filter bank receivers.

ACKNOWLEDGMENT

The author is indebted to Mr. G. T. Flynn, for his valued recommendations, Mr. A. J. Yakutis, who provided necessary equipment and suggestions, and to all my colleagues who helped in the preparation of this note. Thanks are also due to Patricia M. Anderson for her patient help in typing this note.

REFERENCES

1. A. J. Giarola and D. R. Jackson, "Wideband Magnetoelastic Frequency-Selective Limiter for VHF," Boeing Internal Doc. D2-125343-1 (March 1967).

2. D. R. Jackson and R. W. Orth, "A Frequency-Selective Limiter Using Nuclear Magnetic Resonance," Proc. IEEE 55, 36-45 (January 1967).

3. T. R. Billeter, "EPR Frequency-Selective Limiter," Proc. IEEE (letters) 56, 370-371 (March 1968).

4. I. T. Ho and A. E. Siegman, "Passive Phase-Distortionless Parametric Limiting with Varactor Diodes," IRE Trans. MTT-9, 459-472 (November 1961).

5. A. J. Giarola, "Theory for the Signal Suppression in Ferrite Frequency-Selective Limiters," Proc. NEC Conf. 22, 42-44 (October 1966).

6. A. J. Giarola, "Third-Order Intermodulation Products in a Ferrite FSL-Two Signal Theory," Proc. IEEE (letters) 55, 36-45 (January 1967).

7. A. L. Kotzebue, "Frequency Selective Limiting," IRE TMTT-10, 516-520 (November 1962).

8. R. E. Tokheim, C. K. Greene, J. C. Hoover, and P. W. Peter, "Non-reciprocal YIG Filter," IEEE Trans. Magnetics MAG-3, 383-391 (September 1967).

9. B. Lax and K. J. Button, Microwave Ferrites and Ferrimagnetics (McGraw-Hill, New York, 1962), p. 680.

10. N. F. Barber and F. Ursell, "The Response of a Resonant System to Gliding Tone," Phil Mag (May 1948).

11. "Spectrum Analysis," Application Note 63, Hewlett-Packard Company.

12. R. W. Orth, "Frequency Selective Limiters and Their Application," IEEE Trans. Electromagnetic Compatibility ECM-10, 2, 273-283 (June 1968).